1.16
Early Solar System Chronology

K. D. McKeegan

University of California, Los Angeles, CA, USA

and

A. M. Davis

University of Chicago, Chicago, IL, USA

1.16.1 INTRODUCTION 2
1.16.1.1 Chondritic Meteorites as Probes of Early Solar System Evolution 2
1.16.1.2 Short-Lived Radioactivity at the Origin of the Solar System 2
1.16.1.3 A Brief History and the Scope of the Present Review 3
1.16.2 DATING WITH ANCIENT RADIOACTIVITY 4
1.16.3 "ABSOLUTE" AND "RELATIVE" TIMESCALES 5
1.16.3.1 An Absolute Timescale for Solar System Formation 5
1.16.3.2 An Absolute Timescale for Chondrule Formation 8
1.16.3.3 An Absolute Timescale for Early Differentiation of Planetesimals 8
1.16.4 THE RECORD OF SHORT-LIVED RADIONUCLIDES IN EARLY SOLAR SYSTEM MATERIALS 9
1.16.4.1 Beryllium-7 9
1.16.4.2 Calcium-41 10
1.16.4.3 Chlorine-36 11
1.16.4.4 Aluminum-26 11
1.16.4.5 Iron-60 16
1.16.4.6 Beryllium-10 18
1.16.4.7 Manganese-53 19
1.16.4.8 Palladium-107 22
1.16.4.9 Hafnium-182 22
1.16.4.10 Iodine-129 23
1.16.4.11 Lead-205 23
1.16.4.12 Niobium-92 23
1.16.4.13 Plutonium-244 and Samarium-146 24
1.16.5 ORIGINS OF THE SHORT-LIVED NUCLIDES IN THE EARLY SOLAR SYSTEM 24
1.16.6 IMPLICATIONS FOR CHRONOLOGY 26
1.16.6.1 Formation Timescales of Nebular Materials 27
1.16.6.2 Timescales of Planetesimal Accretion and Early Chemical Differentiation 29
1.16.7 CONCLUSIONS 30
1.16.7.1 Implications for Solar Nebula Origin and Evolution 30
1.16.7.2 Future Directions 31
ACKNOWLEDGMENTS 32
REFERENCES 32

1.16.1 INTRODUCTION

1.16.1.1 Chondritic Meteorites as Probes of Early Solar System Evolution

The evolutionary sequence involved in the formation of relatively low-mass stars, such as the Sun, has been delineated in recent years through impressive advances in astronomical observations at a variety of wavelengths, combined with improved numerical and theoretical models of the physical processes thought to occur during each stage. From the models and the observational statistics, it is possible to infer in a general way how our solar system ought to have evolved through the various stages from gravitational collapse of a fragment of a molecular cloud to the accretion of planetary-sized bodies (e.g., Cameron, 1995; Shu *et al.*, 1987; André *et al.*, 2000; Alexander *et al.*, 2001; see Chapters 1.04, 1.17, and 1.20). However, the details of these processes remain obscured, literally, from an astronomical perspective, and the dependence of such models on various parameters requires data to constrain the specific case of our solar system's origin.

Fortunately, the chondritic meteorites sample aspects of this evolution. The term "chondrite" (or chondritic) was originally applied to meteorites-bearing chondrules, which are approximately millimeter-sized solidified melt droplets consisting largely of mafic silicate minerals and glass commonly with included metal or sulfide. However, the meaning of chondritic has been expanded to encompass all extraterrestrial materials that are "primitive," that is, are undifferentiated samples having nearly solar elemental composition. Thus, the chondrites represent a type of cosmic sediment, and to a first approximation can be thought of as "hand samples" of the condensable portion of the solar nebula. The latter is a general term referring to the phase(s) of solar system evolution intermediate between molecular cloud collapse and planet formation. During the nebular phase, the still-forming Sun was an embedded young-stellar object (YSO) enshrouded by gas and dust, which was distributed first in an extended envelope that later evolved into an accretion disk that ultimately defined the ecliptic plane. The chondrites agglomerated within this accretion disk, most likely close to the position of the present asteroid belt from whence meteorites are currently derived. In addition to chondrules, an important component of some chondrites are inclusions containing refractory oxide and silicate minerals, so-called calcium- and aluminum-rich inclusions (CAIs) that also formed as free-floating objects within the solar nebula (see Chapter 1.08). These constituents are bound together by a "matrix" of chondrule fragments and fine-grained dust (which includes a tiny fraction of dust grains that predate the solar nebula; see Chapter 1.02). It is important to realize that, although these materials accreted together at a specific time in some planetesimal, the individual components of a given chondrite can, and probably do, sample different places and/or times during the nebular phase of solar system formation. Thus, each grain in one of these cosmic sedimentary rocks potentially has a story to tell regarding aspects of the early evolution of the solar system.

Time is a crucial parameter in constructing any story. Understanding of relative ages allows placing events in their proper sequence, and measures of the duration of events are critical to developing an understanding of the process. If disparate observations can be related temporally, then structure (at any one time) and evolution of the solar system can be better modeled; or, if a rapid succession of events can be inferred, it can dictate a cause and effect relationship. This chapter is concerned with understanding the timing of different physical and chemical processes that occurred in the solar nebula and possibly on early accreted planetesimals that existed during the nebula stage. These events are "remembered" by the components of chondrites and recorded in the chemical, and especially, isotopic compositions of the host mineral assemblages; the goal is to decide which events were witnessed by these ancient messengers and to decipher those memories recorded long ago.

1.16.1.2 Short-Lived Radioactivity at the Origin of the Solar System

The elements of the chondritic meteorites, and hence of the terrestrial planets, were formed in previous generations of stars. Their relative abundances represent the result of the general chemical evolution of the galaxy, possibly enhanced by recent local additions from one or more specific sources just prior to collapse of the solar nebula $\sim$4.56 Ga. A volumetrically minor, but nevertheless highly significant part of this chemical inventory, is comprised of radioactive elements, from which this age estimate is derived. The familiar long-lived radionuclides, such as ^{238}U, ^{235}U, ^{232}Th, ^{87}Rb, ^{40}K, and others, provide the basis for geochronology and the study of large-scale differentiation amongst geochemical reservoirs over time (see Chapter 1.27). They also provide a major heat source to drive chemical differentiation on a planetary scale (e.g., terrestrial plate tectonics).

A number of short-lived radionuclides also existed at the time that the Sun and the rocky bits of the solar system were forming (Table 1). These nuclides are sufficiently long-lived that they could exist in appreciable quantities in the earliest solar system rocks, but their mean lives are short enough that they are now completely decayed from their primordial abundances. In this sense they are referred to as extinct nuclides. Although less familiar than the still-extant radionuclides, these short-lived isotopes potentially play similar roles: their relative abundances can, in principle, form the basis of various chronometers that constrain the timing of early chemical fractionations, and the more abundant radioisotopes can possibly provide sufficient heat to drive differentiation (i.e., melting) of early accreted planetesimals. The very rapid rate of decay of the short-lived isotopes, however, means that inferred isotopic differences translate into relatively short amounts of time, that is, these potential chronometers have inherently high precision (temporal resolution). The realization of these possibilities is predicated upon understanding the origin(s) and distributions of the now-extinct radioactivity. While this is a comparatively easy task for the long-lived, still existing radionuclides, it poses a significant challenge for the studies of the early solar system. However, this represents the best chance at developing a quantitative high-resolution chronology for events in the solar nebula and, moreover, the question of the origins of the short-lived radioactivity has profound implications for the mechanisms of formation of the solar system (as being, possibly, quite different from that for solar-mass stars in general).

1.16.1.3 A Brief History and the Scope of the Present Review

That short-lived radioactive isotopes existed in the early solar system has been known since the 1960s, when ^{129}Xe excesses were first shown to be correlated with the relative abundance of iodine, implicating the former presence of its parent nuclide, ^{129}I (Jeffery and Reynolds, 1961). Because the half-life of ^{129}I ($\sim$16 Myr) is not so short, its presence in the solar system can be understood as primarily a result of the ambient, quasisteady-state abundance of this nuclide in the parental molecular cloud due to continuous r-process nucleosynthesis in the galaxy (Wasserburg, 1985). The situation changed dramatically in the mid-1970s when it was discovered that CAIs from the Allende meteorite exhibited apparent excesses of ^{26}Mg

Table 1 Short-lived radioactive nuclides once existing in solar system objects.

Fractionation[a]	*Parent nuclide*	*Half-life*[b]	*Daughter nuclide*	*Estimated initial solar system abundance*	*Objects found in*	*References*
Neb	^{7}Be	53.1 days	^{7}Li	10^{-3} ^{9}Be	CAIs	(1)
Neb	^{41}Ca	102 kyr	^{41}K	10^{-8} ^{40}Ca	CAIs	(2)
Plan	^{36}Cl	301 kyr	^{36}S, ^{36}Ar	($\sim 4 \times 10^{-6}$) ^{35}Cl	CAIs, chondrites	(3)
Neb	^{26}Al	717 kyr	^{26}Mg	(6.33×10^{-5}) ^{27}Al	CAIs, chondrules, achondrite	(4)
Neb, Plan	^{60}Fe	1.5 Myr	^{60}Ni	(~ 5–10×10^{-7}) ^{56}Fe	Achondrites, chondrites	(6)
Neb	^{10}Be	1.51 Myr	^{10}B	($\sim 1.0 \times 10^{-3}$) ^{9}Be	CAIs	(5)
Neb, Plan	^{53}Mn	3.74 Myr	^{53}Cr	(1.0×10^{-5}) ^{55}Mn	CAIs, chondrules, carbonates, achondrites	(7)
Plan	^{107}Pd	6.5 Myr	^{107}Ag	($\sim 5 \times 10^{-5}$) ^{108}Pd	Iron meteorites, pallasites	(8)
Plan	^{182}Hf	8.90 Myr	^{182}W	(1.07×10^{-4}) ^{180}Hf	Planetary differentiates	(9)
Plan	^{129}I	15.7 Myr	^{129}Xe	10^{-4} ^{127}I	Chondrules, secondary minerals	(10)
Plan	^{205}Pb	17.3 Myr	^{205}Tl	(~ 1–2×10^{-4}) ^{204}Pb	Iron meteorites	(11)
Plan	^{92}Nb	34.7 Myr	^{92}Zr	10^{-4} ^{93}Nb	Chondrites, mesosiderites	(12)
Plan	^{244}Pu	80.0 Myr	Fission products	(7×10^{-3}) ^{238}U	CAIs, chondrites	(13)
Plan	^{146}Sm	103 Myr	^{142}Nd	(9×10^{-4}) ^{147}Sm	Chondrites	(14)

References: (1) Chaussidon *et al.* (2006); (2) Srinivasan *et al.* (1994, 1996); (3) Lin *et al.* (2005), Hsu *et al.* (2006); (4) Bizzarro *et al.* (2004, 2005a), this work; (5) Chaussidon *et al.* (2006), this work; (6) Mostefaoui *et al.* (2005), Tachibana *et al.* (2006); (7) Dauphas *et al.*, 2005; (8) Chen and Wasserburg (1990); (9) Kleine *et al.* (2005a); (10) Jeffery and Reynolds (1961); (11) Nielsen *et al.* (2006); (12) Schönbachler *et al.* (2002); (13) Hudson *et al.* (1988); (14) Lugmair *et al.* (1983).

[a]Environment in which most significant parent–daughter fractionation processes occur. [b]Half-lives from National Nuclear Data Center, Brookhaven National Laboratory (National Nuclear Data Center, 2006).

(Gray and Compston, 1974; Lee and Papanastassiou, 1974) and that the degree of excess ^{26}Mg correlated with Al/Mg in CAI mineral separates (Lee *et al.*, 1976) in a manner indicative of the *in situ* decay of ^{26}Al ($t_{1/2} = 0.73$ Myr).

The high abundance inferred for this short-lived isotope ($\sim 5 \times 10^{-5}$ ^{27}Al) demanded that it had been produced within a few million years of CAI formation, possibly in a single stellar source, which "contaminated" the nascent solar system with freshly synthesized nuclides (Wasserburg and Papanastassiou, 1982). Because of the close time constraints an attractively parsimonious idea arose, whereby the very same dying star that threw out new radioactivity into the interstellar medium may also have served to initiate gravitational collapse of the molecular cloud fragment that would become the solar system, through the shock wave created by its expanding ejecta (Cameron and Truran, 1977). An alternative possibility that the new radioactive elements were produced "locally" through nuclear reactions between energetic solar particles and the surrounding nebular material was also quickly recognized (Heymann and Dziczkaniec, 1976; Clayton *et al.*, 1977; Lee, 1978). However, many of the early models were unable to produce sufficient amounts of ^{26}Al by irradiation within the constraints of locally available energy sources and the lack of correlated isotopic effects in other elements (see discussion in Wadhwa and Russell, 2000). Almost by default, "external seeding" scenarios and the implied supernova trigger became the preferred class of models for explaining the presence of ^{26}Al and its distribution in chondritic materials.

In the intervening 30 years, as indicated in Table 1, many other short-lived isotopes have been found to have existed in early solar system materials. Several of these have been discovered in recent years, and the record of the distribution of ^{26}Al and other nuclides in a variety of primitive and evolved materials has been documented with much greater clarity. Significant progress has been made since the first edition of this chapter was written. It now seems that both stellar and local production are necessary to explain the full range of short-lived radionuclide abundances. In part due to improvements in mass spectrometry, new data are being generated at an increasing pace, and in some cases, interpretations that seemed solid only a short time ago are now being revised. For further details, the reader is directed to several excellent reviews (Wasserburg, 1985; Swindle *et al.*, 1996; Podosek and Nichols, 1997; Gilmour, 2000; Wadhwa and Russell, 2000; Russell *et al.*, 2001; Kita *et al.*, 2005; Wadhwa *et al.*, 2006a, b).

Development of a quantitative understanding of the source, or sources, of the now-extinct radionuclides is important for constraining the distribution of these radioactive species throughout the early solar system and, thus, is critical for chronology. For the major part of this review, we will tacitly adopt the prevailing point of view, namely that external seeding for the most important short-lived isotopes dominates over possible local additions from nuclear reactions with energetic particles associated with the accreting Sun. This approach permits examination of timescales for self-consistency with respect to major chemical or physical "events" in the evolution of the solar system; the issues of the scale of possible isotopic heterogeneity within the nebula and assessment of local irradiation effects will be explicitly addressed following an examination of the preserved record.

1.16.2 DATING WITH ANCIENT RADIOACTIVITY

In "normal" radioactive dating, the chemical fractionation of a parent isotope from its radiogenic daughter results, after some decay of the parent, in a linear correlation of excesses of the daughter isotope with the relative abundance of the parent. For a cogenetic assemblage, such a correlation is an isochron and its slope permits the calculation of the time since the attainment of isotopic closure, that is, since all relative transport of parent or daughter isotopes effectively ceased. If the fractionation event is magmatic, and the rock quickly cooled, then this time corresponds to an absolute crystallization age.

In a manner similar to dating by long-lived radioisotopes, the former presence of short-lived radioactivity in a sample is demonstrated by excesses of the radiogenic daughter isotope that correlate with the inferred concentration of the parent. However, because the parent isotope is extinct, a stable isotope of the respective parent element must serve as a surrogate with the same geochemical behavior (see Wasserburg, 1985; figure 2). The correlation line yields the initial concentration of radioactive parent relative to its stable counterpart and may represent an isochron; however, its interpretation in terms of "age" for one sample relative to another requires an additional assumption. The initial concentrations of a short-lived radionuclide among a suite of samples can correspond to relative ages only if the samples are all derived from a reservoir that at one time had a uniform

concentration of the radionuclide. Under these conditions, differences in concentration correspond to differences in time only. As before, if the fractionation event corresponds to mineral formation and isotopic closure is rapidly achieved and maintained, then relative crystallization ages are obtained.

One further complication potentially arises that is unique to the now-extinct nuclides. In principle, excesses of a radiogenic daughter isotope could be ''inherited'' from an interstellar (grain) component, in a manner similar to what is known to have occurred for some stable isotope anomalies in CAIs and other refractory phases of chondrites (e.g., Begemann, 1980; Niederer *et al.*, 1980; Niemeyer and Lugmair, 1981; Fahey *et al.*, 1987). In such a case, the correlation of excess daughter isotope with radioactive parent would represent a mixing line rather than *in situ* decay from the time of last chemical fractionation. Such ''fossil'' anomalies (in magnesium) have, in fact, been documented in *bona fide* presolar grains (Zinner, 1998; see Chapter 1.02). These grains of SiC, graphite, and corundum crystallized in the outflows of evolved stars, incorporating very high abundances of newly synthesized radioactivity with $^{26}Al/^{27}Al$ sometimes approaching unity. However, because these grains did not form in the solar nebula from a uniform isotopic reservoir, there is no chronological constraint that can be derived. Probably, the radioactivity in such grains decayed during interstellar transit, and hence arrived in the solar nebula as a ''fossil.''

Even before the discovery of presolar materials, Clayton championed a fossil origin for the magnesium isotope anomalies in CAIs in a series of papers (e.g., Clayton, 1982, 1986). A significant motivation for proposing a fossil origin was, in fact, to obviate chronological constraints derived from Al–Mg systematics in CAIs that apparently required a late injection and fast collapse timescales along with a long (several million years) duration of small dust grains in the nebula. Although some level of inheritance may be present, and can possibly even be the dominant signal in a few rare samples or for specific isotopes (discussed below), for the vast majority of early solar system materials it appears that most of the inventory of short-lived isotopes did indeed decay following mineral formation in the solar nebula. MacPherson *et al.* (1995) summarized the arguments against a fossil origin for the ^{26}Mg excesses in their comprehensive review of the Al–Mg systematics in early solar system materials. In addition to the evidence regarding chemical partitioning during igneous processing of CAIs, the number of short-lived isotopes known (Table 1) and a general consistency of the isotopic records in a wide variety of samples must now be added. The new observations buttress the previous conclusions of MacPherson *et al.* (1995), such that the overwhelming consensus of current opinion is that correlation lines indicative of the former presence of the now-extinct isotopes are truly isochrons representing *in situ* radioactive decay. This is a necessary, but not sufficient, condition for developing a chronology based on these systems.

1.16.3 "ABSOLUTE" AND "RELATIVE" TIMESCALES

To tie high-resolution relative ages to an ''absolute'' chronology, a correlation must be established between the short- and long-lived chronometers, that is, the ratio of the extinct nuclide to its stable partner isotope must be established at some known time (while it was still alive). This time could correspond to the ''origin of the solar system,'' which, more precisely defined, means the crystallization age of the first rocks to have formed in the solar system, or it could refer to some subsequent well-defined fractionation event, for example, large-scale isotopic homogenization and fractionation occurring during planetary melting and differentiation. Both approaches for reconciling relative and absolute chronologies have been investigated in recent years, for example, utilizing the ^{26}Al–^{26}Mg and Pb–Pb systems in CAIs and chondrules for constraining the timing and duration of events in the nebula, and the ^{53}Mn–^{53}Cr and Pb–Pb systems in differentiated meteorites to pin the timing of early planetary melting. The consistency of the deduced chronologies may be evaluated to give confidence (or not) that the assumptions necessary for a temporal interpretation of the record of short-lived radioactivity are, indeed, fulfilled.

1.16.3.1 An Absolute Timescale for Solar System Formation

The early evolution of the solar system is characterized by significant thermal processing of original presolar materials. This processing typically results in chemical fractionation that may potentially be dated by isotopic means in appropriate samples, for example, nebular events such as condensation or distillation fractionate parent and daughter elements according to differing volatility. Likewise, chemical differentiation during melting and segregation

leads to unequal rates of radiogenic ingrowth in different planetary reservoirs (e.g., crust, mantle, and core) that can constrain the nature and timing of early planetary differentiation. Several long-lived and now-extinct radioisotope systems have been utilized to delineate these various nebular and parent-body processes; however, it is only the U–Pb system that can record the absolute ages of the earliest volatility-controlled fractionation events, corresponding to the formation of the first refractory minerals, as well as the timing of melt generation on early planetesimals with sufficiently high precision as to provide a quantitative link to the short-lived isotope systems.

The U–Pb system represents the premier geochronometer because it inherently contains two long-lived isotopic clocks that run at different rates: ^{238}U decays to ^{206}Pb with a half-life of 4,468 Myr, and ^{235}U decays to ^{207}Pb with a much shorter half-life of 704 Myr. This unique circumstance provides a method for checking isotopic disturbance (by either gain or loss of uranium or lead) that is revealed by discordance in the ages derived from the two independent isotopic clocks with the same geochemical behavior (Wetherill, 1956; Tera and Wasserburg, 1972). Such an approach is commonly used in evaluating the ages of magmatic or metamorphic events in terrestrial samples. For obtaining the highest precision ages of volatility-controlled fractionation events in the solar nebula, the U–Pb concordance approach is of limited utility, however, and instead one utilizes ^{207}Pb/^{206}Pb and ^{204}Pb/^{206}Pb variations in a suite of cogenetic samples to evaluate crystallization ages. The method has a significant analytical advantage since only isotope ratios need to be determined in the mass spectrometer, but equally important is the high probability that the age obtained represents a true crystallization age, because the system is relatively insensitive to recent gain or loss of lead (or, more generally, recent fractionation of U/Pb). Moreover, this age is fundamentally based on the isotopic evolution of uranium, a refractory element whose isotopic composition is thought to be invariant throughout the solar system (Chen and Wasserburg, 1980, 1981), and the radiogenic ^{207}Pb/^{206}Pb evolves rapidly at 4.5 Ga because of the relatively short half-life of ^{235}U. In principle, ancient lead loss or redistribution (e.g., owing to early metamorphic or aqueous activity on asteroids, the parent bodies of meteorites) can confound the interpretation of lead isotopic ages as magmatic ages, but such closure effects are usually considered to be insignificant for the most primitive meteorite samples. Whether or not this is a valid assumption is an issue that is open to experimental assessment and interpretation (see discussions in Tilton, 1988 and Tera and Carlson, 1999). The Pb–Pb method can have precisions of 0.5–1.0 Myr in favorable cases using the most advanced current techniques (Amelin, 2006). There are uncertainties in the decay constants of the uranium isotopes that give an uncertainty of 9.3 Myr for early solar system ages. These uncertainties are not included when Pb–Pb ages are quoted. This is not a problem when comparing relative chronologies determined by Pb–Pb with those from short-lived chronometers, but needs to be considered when comparing absolute Pb–Pb ages with those determined from other long-lived chronometers (Amelin, 2006). One further potential complication of the U–Pb system is the possible presence of extinct ^{247}Cm in the early solar system. This isotope decays to ^{235}U by three α- and two β-decays and could perturb Pb–Pb ages. A recent high-precision study by Stirling *et al.* (2005) has established that ^{235}U/^{238}U ratios in bulk meteorites are uniform to within 2 ε units (parts in 10^4), so the precision of Pb–Pb dates for the early solar system remains robust.

Absolute crystallization ages have been calculated for refractory samples, CAIs that formed with very high depletions of volatile lead, by modeling the evolution of ^{207}Pb/^{206}Pb from primordial common (i.e., unradiogenic) lead found in early formed sulfides from iron meteorites. Such ''model ages'' can be determined with good precision (typically a few million years ago), but accuracy depends on the correctness of the assumption of the isotopic composition of initial lead. Sensitivity to this correction is relatively small for fairly radiogenic samples such as CAIs where almost all the lead is due to *in situ* decay, nevertheless, depending on the details of data reduction and sample selection, even the best early estimates of Pb–Pb model ages for CAI formation ranged over $\sim$15 Ma, from 4,553 to 4,568 Ma, with typical uncertainties in the range of 4–5 Ma (see discussions in Tilton, 1988 and Tera and Carlson, 1999). By progressively leaching samples to remove contaminating lead (probably introduced from the meteorite matrix), Allègre *et al.* (1995) were able to produce highly radiogenic (^{206}Pb/^{204}Pb > 150) fractions from four CAIs from the Allende CV3 chondrite, which yielded Pb–Pb model ages of 4,566 $\pm$ 2 Ma. Accuracy problems associated with initial lead corrections can also be addressed by an isochron approach where no particular composition of common lead needs to be assumed, only that a suite of samples are cogenetic and incorporated varying amounts of the same initial lead on crystallization (Tera and Carlson, 1999).

Utilizing this approach, Tera and Carlson (1999) reinterpreted previous lead isotopic data obtained on nine Allende coarse-grained CAIs that had indicated a spread of ages (Chen and Wasserburg, 1981) to instead fit a single lead isochron of age equal to 4,566 ± 8 Ma which, however, is evolved from an initial lead isotopic composition that is unique to CAIs. More recently, Amelin *et al.* (2002) used the isochron method to determine absolute ages of formation for two CAIs from the Efremovka CV3 carbonaceous chondrite. Both samples are consistent with a mean age of 4,567.2 ± 0.6 Ma (Figure 1). Amelin *et al.* (2006) reported further isotopic analyses on one of the two Efremovka CAIs, E60, refining the age to 4,567.11 ± 0.16 Ma, which is the most precise absolute age obtained on CAIs. Because the previous best ages on Allende CAIs are consistent, within their relatively larger errors, with this new lead isochron age we adopt this value of 4,567.11 ± 0.16 Ma as the best estimate for the absolute formation age for coarse-grained (igneous) CAIs from CV chondrites. There is an alternative view; however, Baker *et al.* (2005) reported high-precision lead and magnesium isotopic data for two angrites, SAH99555 and NWA1296, that showed a Pb–Pb age only 1.0 ± 0.6 Myr younger than the Amelin *et al.* (2006) CAI age. Magnesium and initial strontium isotopic compositions indicate a time difference of 3.3–3.8 Myr between CAI formation and angrite formation. Baker *et al.* (2005) suggested that CAI leachates, which are dominated by lead introduced during terrestrial exposure, should be used to represent the common lead component in Efremovka E60, which would change the Pb–Pb age to 4,569.5 ± 0.4 Ma. Thus, further lead isotope work on the absolute formation age of CAIs remains to be done before this age can be considered to be robust.

To the extent that this high-precision, high-accuracy result represents the absolute age of crystallization of CAIs generally, it provides a measure of the age of formation of the solar system since several lines of evidence, in addition to the absolute Pb–Pb ages, indicate that CAIs are the first solid materials to have formed in the solar nebula (for a review, see Podosek and Swindle, 1988). In fact, it is the relative abundances of the short-lived radionuclides, especially ^{26}Al, which provides the primary indication that CAIs are indeed these first local materials. Other evidence is more circumstantial, for example, the prevalence of large stable isotope anomalies in CAIs compared with other materials of solar system

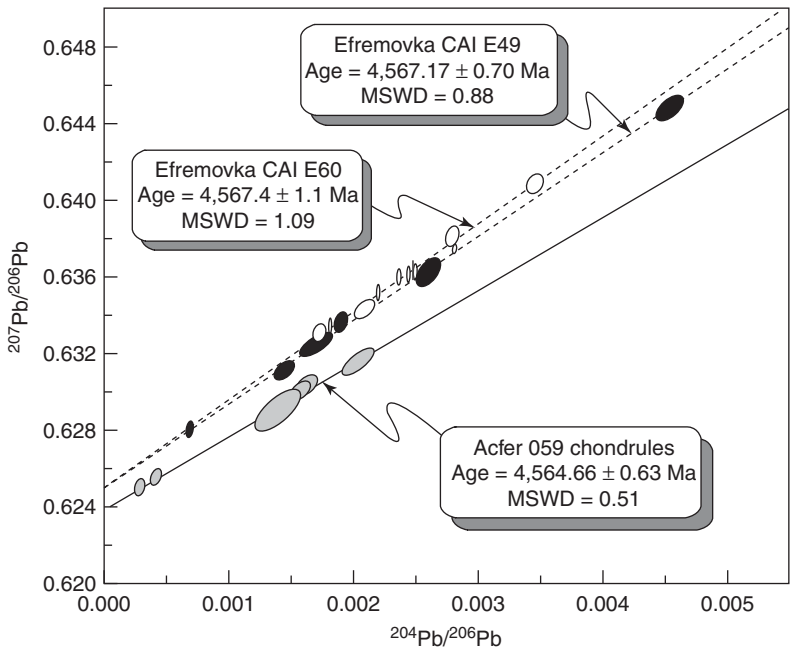

Figure 1 Pb–Pb isochrons for acid-washed fractions of two CAIs from CV3 Efremovka and for the six most radiogenic fractions of acid-washed chondrules from the CR chondrite Acfer 059. The ^{207}Pb/^{206}Pb data are not corrected for any assumed common lead composition; 2σ error ellipses are shown. Isochron ages for the two CAIs overlap with a weighted mean age of 4,567.2 ± 0.6 Ma, which is ~2.5 Myr older than the chondrules. Data and figure reproduced from Amelin *et al.* (2002).

origin (see Chapter 1.08). We will return to the issue of antiquity of CAIs when we examine the distribution of short-lived isotopes among different CAI types.

Other volatility-controlled, long-lived parent–daughter isotope systems (e.g., Rb–Sr) yield absolute ages that are compatible with the coupled U–Pb systems, albeit with poorer precision. Because the chondrites are unequilibrated assemblages of components that may not share a common history, whole-rock or even mineral separate "ages" are not very meaningful for providing a very useful constraint on accretion timescales. High-precision age determinations, approaching 1 Ma resolution, can in principle be obtained from initial $^{87}Sr/^{86}Sr$ in low Rb/Sr phases, such as CAIs (e.g., Podosek *et al.*, 1991). However, such ages depend on deriving an accurate model of the strontium isotopic evolution of the reservoir from which these materials formed. The latter is a very difficult requirement, because it is not likely that a strictly chondritic Rb/Sr ratio was always maintained in the nebular regions from which precursor materials that ultimately formed CAIs, chondrules, and other meteoritic components condensed. Thus, initial strontium "ages," while highly precise, may be of little use in terms of quantitatively constraining absolute ages of formation of individual nebular objects and are best interpreted as only providing a qualitative measure of antiquity (Podosek *et al.*, 1991). It is possible that initial $^{87}Sr/^{86}Sr$ ratios of similar nebular components, for example, type B CAIs, could provide relative formation ages under the assumption that such objects share a common long-term Rb/Sr heritage; however, this has not yet been demonstrated.

1.16.3.2 An Absolute Timescale for Chondrule Formation

Although chondrule formation is thought to be one of the most significant thermal processes to have occurred in the solar nebula, in the sense of affecting the majority of planetary materials in the inner solar system (see Chapter 1.07), the mechanism(s) responsible remains hotly debated after many years of investigation. Similarly, it has long been recognized that obtaining good measurements of chondrule ages would be extremely useful for possibly constraining formation mechanisms and environments, as well as setting important limits on the duration of the solar nebula and, thus, on accretion timescales. However, determination of crystallization ages of chondrules is very difficult because their mineralogy is typically not amenable to large parent–daughter fractionation. Several short-lived isotope systems (discussed below) have been explored in recent years to try to delimit relative formation times for chondrules, for example, compared with CAIs, but high-precision absolute Pb–Pb ages have been measured for only a single meteorite. Amelin *et al.* (2002) used aggressive acid washing of a suite of chondrules from the unequilibrated CR chondrite Acfer 059 to remove unradiogenic lead (from both meteorite matrix and terrestrial contamination). Isochron ages ranged from 4,563 to nearly 4,565 Ma, with a preferred value of $4{,}564.7 \pm 0.6$ Ma (Figure 1) for six of the most radiogenic samples ($^{206}Pb/^{204}Pb > 395$). It is argued that this result dates chondrule formation because lead-closure effects are thought to be insignificant for these pristine samples. If these CR chondrules are representative of chondrules generally, then the data of Amelin *et al.* (2002) imply an interval of ~ 2.5 Ma between the formation of CV CAIs and chondrules in the nebula. Krot *et al.* (2005) reported Pb–Pb ages for chondrules from the CB_a chondrite Gujba ($4{,}562.7 \pm 0.5$ Ma) and CB_b chondrite Hammadah al Hamra 257 ($4{,}562.8 \pm 0.9$ Ma). These ages are ~ 5 Myr younger than CAIs. Krot *et al.* (2005) argued that this time difference was too great for nebular processes and suggested that CB chondrite chondrules were formed in a giant impact between planetary embryos.

1.16.3.3 An Absolute Timescale for Early Differentiation of Planetesimals

Time markers for tying short-lived chronometers to an absolute timescale can potentially be provided by early planetary differentiates. The basic requirements are that appropriately ancient samples would have to have evolved from a reservoir (magma) that had achieved isotopic equilibrium with respect to daughter elements of both long- and short-lived systems (i.e., lead and chromium or magnesium, respectively), then cooled rapidly following crystallization, and remained isotopically closed until analysis in the laboratory. In practice, the latter requirement means that samples should be undisturbed by shock and free of terrestrial contamination. No sample is perfect in all these respects, but the angrites are considered to be nearly ideal (the major problem being terrestrial lead contamination). By careful cleaning, Lugmair and Galer (1992) determined high-precision Pb–Pb model ages for the angrites Lewis Cliff 86010 (LEW) and Angra dos Reis (ADOR). The results are concordant in U/Pb

and with other isotopic systems as well as with each other, and provide an absolute crystallization age of 4,557.8 ± 0.5 Ma for the angrites (Lugmair and Galer, 1992). This is a significant time marker (“event”) because angrite mineralogy also provides large Mn/Cr fractionation that is useful for accurate $^{53}Mn/^{55}Mn$ determination. Baker *et al.* (2005) reported a highly precise and ancient Pb–Pb age for the Sahara 99555 angrite of 4,566.2 ± 0.1 Ma, indicating crystallization of basalt on the surface of the angrite parent body only 1 Myr after the formation of CAIs. Amelin *et al.* (2006) reported a Pb–Pb age for the Asuka 881394 eucrite of 4,566.52 ± 0.33 Ma, only 0.59 ± 0.36 Myr after CAI formation.

The eucrites are highly differentiated (basaltic) achondrites that, along with the related howardites and diogenites, may have originated from the asteroid 4 Vesta (Binzel and Xu, 1993; see Chapter 1.11). Unfortunately, the U/Pb systematics of eucrites appear to be disturbed, yielding Pb–Pb ages up to ~220 Myr younger than angrites (Galer and Lugmair, 1996). This compromises the utility of the eucrites as providing independent tie points between long- and short-lived chronometers.

Evidence for an extended thermal history of equilibrated ordinary chondrites is provided by U–Pb analyses of phosphates (Göpel *et al.*, 1994). The phosphates (merrillite and apatite) are metamorphic minerals produced by the oxidation of phosphorus originally present in metal grains. Phosphate mineral separates obtained from chondrites of metamorphic grade 4 and greater have Pb–Pb model ages (Göpel *et al.*, 1994) from 4,563 (for H4, Ste. Marguerite) to 4,502 Ma (for H6, Guareña). The oldest ages are nearly equivalent to Pb–Pb ages from CR chondrules (Amelin *et al.*, 2002) and only a few million years younger than CAIs, indicating that accretion and thermal processing was rapid for the H4 chondrite parent body. The relatively long time interval of ~60 Myr has implications for the nature of the H chondrite parent body and the heat sources responsible for long-lived metamorphism (Göpel *et al.*, 1994).

1.16.4 THE RECORD OF SHORT-LIVED RADIONUCLIDES IN EARLY SOLAR SYSTEM MATERIALS

Here, we discuss the evidence for the prior existence of the now-extinct isotopes in meteoritic materials and, in the better-studied cases, what is known about the distribution of that isotope in the early solar system. Table 1 summarizes the basic facts regarding those short-lived radioisotopes that are unequivocally known to have existed as live radioactivity in rocks formed in the early solar system and provides an estimate of their initial abundances compared with a reference isotope. The table is organized in terms of increasing half-life and according to the main environment for parent–daughter chemical fractionation. The latter property indicates what types of events can potentially be dated and largely dictates what types of samples record evidence that a certain radioisotope once existed. Note that there is only a small degree of overlap demonstrated thus far for a few of the isotope systems. For example, it is well-documented that the Mn–Cr system is sensitive to fractionation in both nebular and parent-body environments and, as we see below, new high-precision magnesium isotopic measurements are making possible application of the Al–Mg system to parent-body processes, but other systems which might similarly provide linkages from the nebula through accretion to early differentiation have not been fully developed due to either analytical difficulties (e.g., Fe–Ni) and/or difficulties in constraining mineral hosts and closure effects (e.g., I–Xe and ^{244}Pu). The initial abundances refer to the origin of the solar system, which, as discussed previously, means the time of CAI formation, and hence these can only be measured directly in nebular samples. The initial abundances of those isotopes that are found only in differentiated meteorites also refer back to the time of CAI formation, but such a calculation necessarily requires a chronological framework and is underpinned by the absolute time markers provided by the Pb–Pb system.

We now describe, in order of half-life, short-lived radionuclides whose presence has been searched for, and in most cases, confirmed, in the early solar system.

1.16.4.1 Beryllium-7

Beryllium-7 decays by electron capture to ^{7}Li with a half-life of 53.3 days. Chaussidon *et al.* (2006) found variations of ~25% in $^{7}Li/^{6}Li$ ratios within an Allende CAI, and suggested that they may be due to *in situ* decay of ^{7}Be. Boron isotopes were also measured in this CAI and it has a well-defined ^{10}Be–^{10}B isochron with a slope corresponding to an initial $^{10}Be/^{9}Be$ ratio of $(1.04 \pm 0.09) \times 10^{-3}$ (see Section 1.16.4.5). There are significant difficulties associated with lithium isotopic measurements in CAIs, in that lithium can be introduced by secondary alteration processes long after the decay of

short-lived ^{7}Be. Chaussidon *et al.* (2006) rejected analyses that did not plot along trajectories expected for closed system crystal fractionation on a Be versus Li concentration plot. There are further difficulties caused by the fact that lithium diffuses very rapidly and can mass fractionate during diffusion (Richter *et al.*, 2004). Corrections also had to be made for spallation production of lithium isotopes by galactic cosmic rays. After correction for these effects and rejection of "contaminated" analyses, Chaussidon *et al.* (2006) inferred an initial ^{7}Be/^{9}Be ratio of 0.0061 ± 0.0013 for Allende CAI 3529-41. In their calculation of the slope of the isochron, they did not weight data points by their uncertainties. A weighted fit gives a slightly higher initial ^{7}Be/^{9}Be ratio of 0.0100 ± 0.0007. The identification of ^{7}Be as a short-lived radionuclide in the early solar system remains tentative, given how large the correction effects are and the necessity of rejecting a significant fraction of the measured data. If ^{7}Be is present, it has profound importance for short-lived radionuclide production within the early solar system. The half-life is so short that it cannot have been produced elsewhere.

1.16.4.2 Calcium-41

Calcium-41 decays by electron capture to ^{41}K with a half-life of only 103 kyr. It has the distinction of being the shortest-lived isotope for which firm evidence exists in early solar system materials, and this fact makes it key for constraining the timescale of last nucleosynthetic addition to solar system matter (in the external seeding scenario). It also makes ^{41}Ca exceedingly difficult to detect experimentally, because it can only be found to have existed in the oldest materials and then in only very small concentrations. Fortunately, its daughter potassium is rather volatile and calcium is concentrated in refractory minerals (the "C" in CAI) leading to large fractionations. Hutcheon *et al.* (1984) found hints for ^{41}Ca in Allende refractory inclusions, but could not clearly resolve ^{41}K excesses above measurement uncertainties.

The first unambiguous evidence of live ^{41}Ca came with the demonstration of correlated excesses of ^{41}K/^{39}K with Ca/K in Efremovka CAIs by Srinivasan *et al.* (1994, 1996). Subsequent measurements by the PRL group have established that ^{41}Ca was also present in refractory oxide phases (hibonite) of CM and CV chondrites (Sahijpal *et al.*, 1998, 2000). The CM hibonite grains are generally too small to permit enough multiple measurements to define an isochron on individual objects, even by ion probe; however, hibonite crystals from Allende CAIs show good correlation lines (Sahijpal *et al.*, 2000) consistent with that found for Efremovka and indicating that ^{41}Ca decayed *in situ*. Most of the isolated CM hibonite grains also show ^{41}K/^{39}K excesses that are consistent with the isochrons obtained on silicate minerals of CAIs, except $\sim 1/3$ of the hibonite grains appear to have crystallized with "dead" calcium (i.e., they have normal ^{41}K/^{39}K compositions). The ensemble isochron (Figure 2) yields an initial value of ^{41}Ca/^{40}Ca $= 1.4 \times 10^{-8}$ with a formal error of $\sim 10\%$ relative and a statistical scatter that is commensurate with the measurement uncertainties. Such a small uncertainty would correspond to a very tight timescale (~ 15 kyr) for the duration of formation of these objects; however, possible systematic uncertainties in the mass spectrometry may increase this interval somewhat. The hibonite grains that contain no excess ^{41}K/^{39}K are unlikely to have lost that signal and, thus, must either have formed well after the other samples, or else they never incorporated live ^{41}Ca during their crystallization. An important clue is that these same grains also never contained ^{26}Al (Sahijpal and Goswami, 1998; Sahijpal *et al.*, 1998, 2000); we will return to the significance of this correlation in discussing the scale of isotopic heterogeneity in the nebula and the

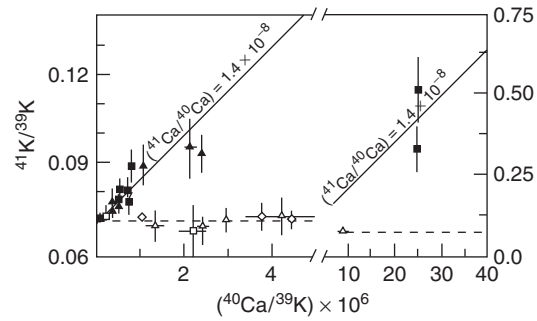

Figure 2 Potassium isotopic compositions measured in individual hibonite grains (Sahijpal *et al.*, 1998) plotted as a function of Ca/K ratio. Hibonite grains from the carbonaceous chondrites Murchison, Allende, and Efremovka, which formed with close to canonical levels of ^{26}Al are indicated as filled symbols, whereas hibonite grains that crystallized with no ^{26}Al are open squares and triangles. Terrestrial standards are plotted as open diamonds; error bars are 1σ. The isochron corresponding to live ^{41}Ca at the level ^{41}Ca/^{40}Ca $= 1.4 \times 10^{-8}$, determined for Efremovka CAIs (Srinivasan *et al.*, 1996), is also shown. Those hibonite grains that contained ^{26}Al are seen to plot on the same ^{41}Ca isochron as the CAIs, but grains lacking ^{26}Al are also lacking ^{41}Ca and plot on the horizontal dashed line corresponding to terrestrial ^{41}K/^{39}K. Data and figure adapted from Sahijpal *et al.* (1998).

source of ^{41}Ca and ^{26}Al. The recent discovery that bulk CAIs lie along an isochron consistent with a somewhat higher ^{26}Al/^{27}Al ratio than that inferred from internal isochrons of individual CAIs raises the possibility that the initial solar system ^{41}Ca/^{40}Ca ratio was higher than the value inferred by Sahijpal *et al.* (1998). The half-life of ^{41}Ca is so short that the early solar system ^{41}Ca/^{40}Ca increases by a factor 10 for each 26% increase in the early solar system ^{26}Al/^{27}Al. Correcting the inference of Sahijpal *et al.* (1998), ^{41}Ca/^{40}Ca $= 1.4 \times 10^{-8}$ for hibonite with canonical ^{26}Al/^{27}Al (5×10^{-5}), to the current best estimate of early solar system ^{26}Al/^{27}Al (6.33×10^{-5}, Table 1) gives initial ^{41}Ca/^{40}Ca ratios of 7×10^{-8}. Further potassium isotope measurements with high-precision magnesium isotopic measurement on CAIs are needed to better constrain this value.

1.16.4.3 Chlorine-36

Chlorine-36 has a half-life of 300 kyr and decays by β-decay (98.1%) to ^{36}Ar and by electron capture and positron emission (1.9%) to ^{36}S. Murty *et al.* (1997) reported ^{36}Ar in the matrix of the Efremovka CV chondrite in excess of the amount expected from trapped and cosmogenic components and attributed it to *in situ* decay of ^{36}Cl. They inferred an initial ^{36}Cl/^{35}Cl ratio of $(1.4 \pm 0.2) \times 10^{-6}$. Lin *et al.* (2005) used an ion microprobe to measure sulfur isotopes in sodalite, a chlorine-bearing mineral commonly found as a secondary alteration product in CAIs and matrix in CV chondrites. They found well-defined isochrons in four sodalite-rich regions in a CAI from the Ningqiang CV chondrite, leading to inferred initial ^{36}Cl/^{35}Cl ratios of $(5\text{–}11) \times 10^{-6}$. From the fact that these areas had ^{26}Al/^{27}Al of $< 5 \times 10^{-6}$, they inferred an initial solar system ^{36}Cl/^{35}Cl ratio of $\geq 1.6 \times 10^{-4}$. Hsu *et al.* (2006) reported a combined ^{36}Cl–^{36}S and ^{26}Al–^{26}Mg study of an altered Allende CAI named the Pink Angel. From the inferred ^{36}Cl/^{35}Cl ratio and the upper limit on ^{26}Al/^{27}Al, they calculated an early solar system ^{36}Cl/^{35}Cl ratio of $> 10^{-3}$. It is not plausible to produce this level of ^{36}Cl in supernovae or AGB stars, so Hsu *et al.* (2006) concluded that ^{36}Cl must have been produced by a late episode of particle bombardment within the solar system.

1.16.4.4 Aluminum-26

Aluminum-26 decays by positron emission and electron capture to ^{26}Mg with a half-life of $\sim$730 kyr. The discovery circumstances of ^{26}Al have already been discussed (Section 1.16.1.3) and since those early measurements, a large body of data has grown to include analyses of CAIs from all major meteorite classes (carbonaceous, ordinary, and enstatite) as well as important groups within these classes (e.g., CM, CV, CH, CR, CO); sparse data also exist for aluminum-rich phases from several differentiated meteorites and in chondrules. Data obtained prior to 1995 were the subject of a comprehensive review by MacPherson *et al.* (1995); for the most part, their analysis relied heavily on the extensive record in the large, abundant CAIs from CV chondrites, although significant numbers of refractory phases from other carbonaceous chondrite groups were also considered. Between that time and the first edition of this chapter, work generally concentrated on extending the database to include smaller CAIs from underrepresented meteorite groups and, especially, chondrules (mostly from ordinary chondrites). Most measurements were performed by ion microprobe because of the need to localize analysis on mineral phases with high Al/Mg ratios to resolve the addition of radiogenic ^{26}Mg*; this capability was particularly important for revealing internal Al–Mg isochrons in chondrules by examining small regions of trapped melt or glassy mesostasis in between the larger ferromagnesian minerals that dominate chondrules (Russell *et al.*, 1996; Kita *et al.*, 2000; McKeegan *et al.*, 2000b; Mostefaoui *et al.*, 2002). There have been two significant technical developments in that past 3 years that have profoundly changed understanding of the Al–Mg system, both of which resulted in much higher precision magnesium isotopic analyses: (1) high-precision isotopic analysis by multicollector inductively coupled plasma mass spectrometry (MC-ICPMS), both on dissolved samples and using laser ablation sampling devices for spot analyses; and (2) multiple collector development on large-radius ion microprobes.

With the new level of precision of magnesium isotopic analyses, additional care must be taken in treating the data. Magnesium has three stable isotopes, ^{24}Mg, ^{25}Mg, and ^{26}Mg. Isotopic mass fractionation of magnesium can occur in nature, during chemical separation of magnesium from samples, and in mass spectrometers. During mass fractionation, the ^{26}Mg/^{24}Mg ratio varies by about twice as much as the ^{25}Mg/^{24}Mg ratio. When magnesium isotopic compositions were measured with precision of $\sim$1‰ or worse, the exact relationship between ^{26}Mg/^{24}Mg fractionation and ^{25}Mg/^{24}Mg fractionation did not matter much when determining the amount of radiogenic

^{26}Mg. However in more recent results with precisions of 0.1‰ or better on samples with low Al/Mg, the fractionation law used becomes important. Isotopic mass fractionation during chemical separation is minimized by ensuring that chemical yields are high; fractionation during mass spectrometry can be corrected using standards of known isotopic composition such that the instrumental mass fractionation law is well calibrated.

Magnesium isotopic compositions are usually expressed in δ notation, i.e., $\delta^{25}\text{Mg} = [(^{25}\text{Mg}/^{24}\text{Mg})_{\text{sample}}/(^{25}\text{Mg}/^{24}\text{Mg})_{\text{standard}} - 1] \times 1{,}000$. On a plot of δ^{25}Mg versus δ^{26}Mg, mass fractionation due to equilibrium fractionation or kinetic effects lie along lines that have a slope of ~ 0.5. Although these relationships appear to be linear over a narrow range of mass fractionation, in fact they are curves. Since most mass fractionation mechanisms are exponential processes, it is convenient to express isotope ratios as another related quantity, $1000 \times \ln[(^{25}\text{Mg}/^{24}\text{Mg})_{\text{sample}}/(^{25}\text{Mg}/^{24}\text{ Mg})_{\text{standard}} - 1]$, denoted as ϕ^{25}Mg by Davis *et al.* (2005) and as δ^{25}Mg′ by Young *et al.* (2005). On a plot of ϕ^{25}Mg versus ϕ^{26}Mg, the different mass fractionation processes plot as straight lines, but with differing slopes depending on the nature of the fractionation process. Fractionation due to the kinetic isotope effect gives a slope of 0.51101 and that due to equilibrium isotope partitioning gives 0.52100 (Young *et al.*, 2002; Davis *et al.*, 2005). Most CAIs have magnesium that is mass-fractionated by a few ‰ amu^{-1} (see Chapter 1.15).

The mass fractionation in CAIs is believed to have been caused by the kinetic isotope effect during high-temperature evaporation in the solar nebula. Davis *et al.* (2005) evaporated melts of CAIs in vacuum and measured magnesium isotopic compositions by MC-ICPMS. On a plot of ϕ^{25}Mg versus ϕ^{26}Mg, their data give a slope of 0.51400 ± 0.00024. Several papers have been published with high-precision magnesium isotopic data, using different slopes to correct for mass fractionation: Bizzarro and coworkers use 0.511, Young and coworkers use 0.521, and McKeegan and coworkers use 0.514. As an example of the effect of these different fractionation laws, consider a spinel grain, with $^{27}\text{Al}/^{24}\text{Mg} = 2.53$, a typical degree of mass fractionation for a CAI, $\delta^{25}\text{Mg} = 5‰$, and an initial $^{26}\text{Al}/^{27}\text{Al}$ value of 6.33×10^{-5} (see below). Excesses or deficits in ^{26}Mg due to ^{26}Al decay are usually expressed as $\Delta^{26}\text{Mg} = \phi^{26}\text{Mg} - \phi^{26}\text{Mg} \times \text{slope}$. In this example, Δ^{26}Mg should be 1.15‰ after complete decay of ^{26}Al. If this is the value obtained with the slope we have adopted, 0.514, recalculating with the kinetic value, 0.511, gives 1.07‰, and the equilibrium value, 0.521, gives 1.26‰. These shifts may seem small, but for an isochron passing through the origin and the spinel in our example, the two slopes would imply initial $^{26}\text{Al}/^{27}\text{Al}$ values of 5.89×10^{-5} and 6.93×10^{-5}, a range of 15% that corresponds to a time difference of 168 kyr. The effect of ϕ^{25}Mg versus ϕ^{26}Mg slope on Δ^{26}Mg depends only on the degree of mass fractionation, not on Al/Mg ratio. It has only become important recently with the development of high-precision magnesium isotopic methods applied to low-Al/Mg samples.

To first order, the larger data set prior to the high-precision measurements extends and confirms the general assessments of MacPherson *et al.* (1995). The distribution of inferred initial $^{26}\text{Al}/^{27}\text{Al}$ in CAIs is bimodal (Figure 3a), with the dominant peak at the so-called canonical value of 4.5×10^{-5}, and a second peak at dead aluminum (i.e., $^{26}\text{Al}/^{27}\text{Al} = 0$). MacPherson *et al.* (1995) demonstrated that this pattern applied to all classes of carbonaceous chondrites, although the relative heights of the two peaks varied among different meteorites (mostly reflecting a difference in CAI types; see Chapter 1.08). The dispersion of the canonical peak (amounting to $\sim 1 \times 10^{-5}$, FWHM) was considered to represent a convolution of measurement error and geologic noise; there was no robust data indicating that any CAIs formed with $(^{26}\text{Al}/^{27}\text{Al})_0$ significantly above the canonical ratio.

The first hint that CAIs formed with $(^{26}\text{Al}/^{27}\text{Al})_0$ significantly above $\sim 5 \times 10^{-5}$ came from the data for one Allende CAI (Galy *et al.*, 2000): a model isochron yields $(^{26}\text{Al}/^{27}\text{Al})_0 = (6.01 \pm 0.22) \times 10^{-5}$ (corrected with a ϕ^{25}Mg versus ϕ^{26}Mg slope of 0.514), which is marginally higher than any previously determined value. Another strong hint came from MC-ICPMS measurements of a number of bulk CAIs, which gave an isochron with a slope corresponding to $(6.85 \pm 0.85) \times 10^{-5}$, reported by Galy *et al.* (2004). These data were collected in two laboratories, each of which used a different mass fractionation law (I. D. Hutcheon, personal communication). Correction of all data to the 0.514 slope yields $(^{26}\text{Al}/^{27}\text{Al})_0 = (6.36 \pm 0.13) \times 10^{-5}$. This work suggested the possibility that nebular fractionation established the bulk Al/Mg ratios of CAIs, but that internal isochrons determined by ion microprobe recorded later remelting events. Bizzarro *et al.* (2004) strongly confirmed this with a very precise isochron computed for a suite of bulk Allende CAIs. Their data are shown in Figure 4, which is a corrected version of their published plot: Bizzarro *et al.* (2005) published an erratum correcting Al/Mg ratios and we have recorrected their magnesium isotopic data for mass

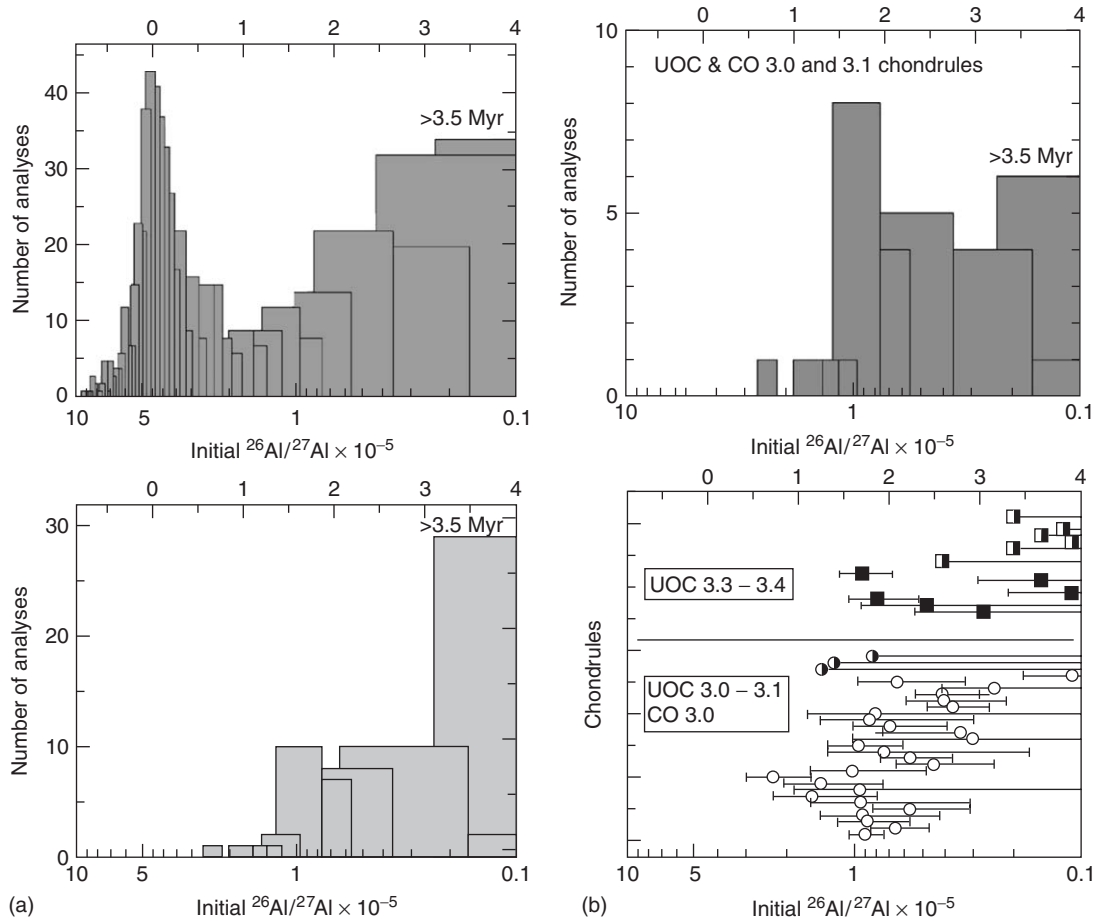

Figure 3 (a) Top panel: Histogram of initial $^{26}Al/^{27}Al$ inferred for CAIs; the number of analyses (taken to be representative of the number of samples) is plotted versus time after CAI formation (top axis), where time 0 is taken as the "canonical" $^{26}Al/^{27}Al = 4.5 \times 10^{-5}$ peak of the distribution for CAIs. In addition to the canonical value, a significant number of CAIs do not preserve any evidence for having formed with live ^{26}Al; samples with only upper limits are summed in the last bin, indicating the achievement of isotopic closure at least 3.5 Myr after time 0, or alternatively, never having incorporated ^{26}Al at all (see text). Data sources are summarized by MacPherson *et al.* (1995). Bottom panel: Similar histogram summarizing data on plagioclase-olivine-inclusions (POIs) and chondrules (both aluminum-rich and ferromagnesian). In contrast to CAIs, there is no peak at $\sim 5 \times 10^{-5}$ and most chondrules show no evidence for having incorporated ^{26}Al. Some chondrules do show evidence for $^{26}Al/^{27}Al$ initial values at the level of $\sim 1 \times 10^{-5}$ or lower, indicating the formation 1.5 to several million years after CAIs. Data sources are those summarized by MacPherson *et al.* (1995), supplemented by more recent data (Russell *et al.*, 1996; Kita *et al.*, 2000; McKeegan *et al.*, 2000b; Huss *et al.*, 2001; Mostefaoui *et al.*, 2002; Hsu *et al.*, 2003; Kunihiro *et al.*, 2004). (b) Top panel: Histogram similar to the bottom panel of (a), except showing the inferred $^{26}Al/^{27}Al$ distribution for only those chondrules from the most unequilibrated meteorites, that is, POIs and chondrules from metamorphic grades >3.1 have been removed from the plot. Also, this plot now shows the number of chondrules with that distribution, as opposed to the number of analyses considering each datum as a model isochron. Chondrules for which ^{26}Mg excesses are not well resolved (i.e., only upper limits are obtained or Al–Mg isochron slopes are within 2σ error of 0) are accumulated in the last histogram bin. A peak in the distribution may be discerned at $^{26}Al/^{27}Al \sim 1 \times 10^{-5}$, which corresponds to 1.5–2 Myr after time 0. Bottom panel: Inferred $^{26}Al/^{27}Al$ ratios for individual ferromagnesian and aluminum-rich chondrules with 2σ errors. Chondrules from the lowest metamorphic grades (3.0, 3.1) of unequilibrated ordinary (LL) and carbonaceous (CO) chondrites are shown in open circles, those from metamorphic grades 3.3 and above are shown in filled squares. Chondrules for which only upper limits are obtained are shown in half-open/half-filled symbols. It is apparent that chondrules from more intensely metamorphosed meteorites display apparently lower $^{26}Al/^{27}Al$ initial values. Among the most unequilibrated samples, an interval of >1 Myr is implied for the duration of chondrule formation. Data sources as in (a).

fractionation using the 0.514 slope (they used 0.511, M. Bizzarro, personal communication). The slope corresponds to $(^{26}Al/^{27}Al)_0 = (6.33 \pm 0.11) \times 10^{-5}$, in remarkable agreement with the Galy *et al.* (2004) value, and we adopt it as the best current estimate of the initial solar system $^{26}Al/^{27}Al$ ratio.

In most ion microprobe measurements of internal isochrons for CAIs, the slope of the isochron is largely determined by analyses of anorthitic plagioclase. This phase is susceptible to mobilization of magnesium during metamorphism (LaTourrette and Wasserburg, 1998) or, possibly, during nebular events (Podosek *et al.*, 1991). However, with the recent availability of high-precision magnesium measurements on other phases, there are now indications of a real spread in initial $^{26}Al/^{27}Al$ ratios within CAIs. Young *et al.* (2005) reported over 200 laser ablation MC-ICPMS analyses of eight CAIs. The data are shown in Figure 5, and are corrected to a ϕ^{25}Mg versus ϕ^{26}Mg slope of 0.514 (Young *et al.* used 0.521). Three things are clear from this data set: (1) most of the points lie above the old canonical $(^{26}Al/^{27}Al)_0$ value of 4.5×10^{-5}; (2) few data points are above the new early solar system $(^{26}Al/^{27}Al)_0$ value of 6.33×10^{-5}; and (3) the data have significant scatter that corresponds to a time period of several times 10^5 years.

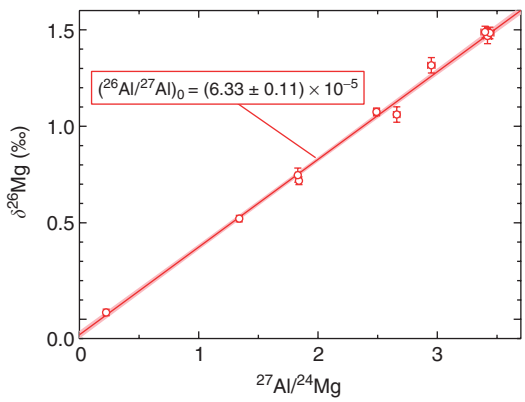

Figure 4 ^{26}Al–^{26}Mg isochron diagram for several Allende CAIs. The data are as reported by Bizzarro *et al.* (2004, 2005), but corrected to ϕ^{25}Mg versus ϕ^{26}Mg slope of 0.514 (see text). This data set provides the best current estimate of the early solar system $^{26}Al/^{27}Al$ ratio, which represents the time of volatility fractionation of aluminum from magnesium in the solar nebula.

High-precision multicollector ion microprobe techniques have been applied recently to a variety of CAIs. These give internal isochrons corresponding to initial $^{26}Al/^{27}Al$ ratios of $3.9–6.26 \times 5$ (Taylor *et al.*, 2005; Cosarinsky *et al.*, 2006; Liu *et al.*, 2006). No ages significantly in excess of the new canonical early solar system $^{26}Al/^{27}Al$ ratio of 6.33×10^{-5} have been found. Some work has also been done on the Wark–Lovering rims commonly found around CAIs (see Chapter 1.08), showing that they formed 0–300 kyr after the interior of

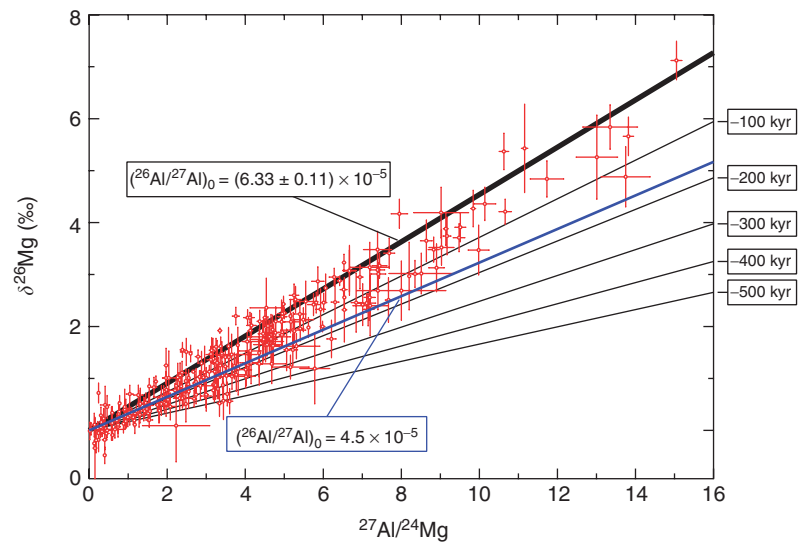

Figure 5 ^{26}Al–^{26}Mg isochron diagram for over 200 laser ablation analysis spots on eight CAIs reported by Young *et al.* (2005) and corrected to ϕ^{25}Mg versus ϕ^{26}Mg slope of 0.514 (see text). Also shown are the best estimate for the early solar system $^{26}Al/^{27}Al$ ratio, 6.33×10^{-5}, an earlier estimate of this ratio, 4.5×10^{-5} (MacPherson *et al.*, 1995), and several isochrons drawn at intervals of 100 kyr younger than the early solar system $^{26}Al/^{27}Al$ ratio. There are no data points significantly above the early solar system $^{26}Al/^{27}Al$ ratio, but there is a distribution below this ratio, implying that these CAIs were recrystallized, perhaps many times, over a few hundred thousand years after initial formation.

the host CAI (Cosarinsky *et al.*, 2005; Simon *et al.*, 2005). A fairly consistent picture appears to be forming: a nebular Al/Mg volatility fractionation occurred at a well-defined time corresponding to the new canonical early solar system $^{26}Al/^{27}Al$ ratio, establishing the bulk CAI isochron of Bizzarro *et al.* (2004) (corrected), followed by several hundred thousand years of reheating events that established internal isochrons of individual CAIs.

The existence of a canonical $(^{26}Al/^{27}Al)_0$ value was previously based on analyses of CAIs only from carbonaceous chondrites; refractory inclusions from ordinary and enstatite chondrites are rare and often very small, and thus few had been discovered and none analyzed. There are now data for four CAIs from unequilibrated ordinary chondrites (Russell *et al.*, 1996; Huss *et al.*, 2001) and for 11 hibonite-bearing inclusions from enstatite chondrites (Guan *et al.*, 2000); all are consistent with $(^{26}Al/^{27}Al)_0$ in the range $\sim(3.5–5.5) \times 10^{-5}$, except for four of the (very small) hibonite grains for which $^{26}Mg^*$ could not be resolved. Thus, the same canonical value characterizes CAIs from all major meteorite classes. The possible meaning of this confirmation in terms of nebular chronology based on ^{26}Al is not completely straightforward, however.

The idea that many CAIs, whether they originally formed by melt crystallization or by condensation, have suffered some degree of disturbance to their Al–Mg isotopic system is well documented via correlated petrographic and isotopic evidence (MacPherson *et al.*, 1995 and references therein). For example, *in situ* isotopic measurements have demonstrated that certain anorthite crystals within a CAI can record resetting events $\sim$1 Myr or more following CAI formation (see figure 28 of Chapter 1.08). In general, it seems to be the large type B CAIs from CV chondrites that are the most prone to have suffered multiple thermal events capable of at least partially resetting the Al–Mg system (Podosek *et al.*, 1991; Caillet *et al.*, 1993; MacPherson and Davis, 1993; MacPherson *et al.*, 1995); the protracted and complex thermal histories of type B CAIs are also evident in other chemical and isotopic systems, particularly the microdistribution of oxygen isotopes within individual inclusions (Clayton and Mayeda, 1984; Young and Russell, 1998; Yurimoto *et al.*, 1998; McKeegan and Leshin, 2001). MacPherson *et al.* (1995) have argued that the trailing distribution of $^{26}Al/^{27}Al$ values downward from the canonical peak primarily represents a protracted period of thermal processing of CAIs, possibly accompanied by secondary mineral formation, over a few million years residence time in the solar nebula. Recently, Hsu *et al.* (2000) documented multiple isochrons within a single type B Allende CAI that they interpreted as signifying three discrete melting events separated in time by a few hundred thousand years. Such observations set lower bounds on the duration of the lifetime of the nebula and of significant heat sources, capable of producing CAIs, within the regions of the nebula.

The duration of high-temperature processes in the solar nebula is closely related to the age difference between CAIs and chondrules, and it is in this area that some of the most significant new data have been developed in recent years. The first evidence for radiogenic $^{26}Mg^*$ in non-CAI material was found in a plagioclase-bearing chondrule from the highly unequilibrated ordinary chondrite Semarkona (Hutcheon and Hutchison, 1989); the isochron implies an initial abundance of $(^{26}Al/^{27}Al)_0 = (7.7 \pm 2.1) \times 10^{-6}$. In most cases, however, only upper limits on ^{26}Al abundances could be determined in a handful of plagioclase grains from chondrules in ordinary chondrites (Hutcheon *et al.*, 1994; Hutcheon and Jones, 1995). Today, initial $^{26}Al/^{27}Al$ ratios have been determined in $\sim$50 chondrules from several unequilibrated ordinary and carbonaceous chondrites. Chondrules with abundant aluminum-rich minerals (plagioclase-rich chondrules) and those with ''normal'' ferromagnesian mineralogy have been analyzed (Figure 3a, bottom panel). Chondrules have distinctly lower $(^{26}Al/^{27}Al)_0$ than CAIs, mostly by a factor of 5 or more. A significant number of chondrules show no resolvable $^{26}Mg^*$, implying that if they evolved from the same canonical $(^{26}Al/^{27}Al)_0$ that characterized the nebular regions where many CAIs formed, then chondrules achieved isotopic closure of the Al–Mg system at least 3–4 Myr (and possibly significantly more) after CAI formation. A closer inspection of the record, however, indicates that those chondrules from meteorites that are more extensively metamorphosed tend to have lower $(^{26}Al/^{27}Al)_0$ values (Figure 3b). This would indicate that metamorphic redistribution, on an asteroid, could be obscuring the nebular record of $^{26}Mg^*$ in these meteorites.

Chondrules that have been analyzed from some of the most pristine meteorites (e.g., Semarkona, Bishunpur, Yamato 81020) tend to show detectable ^{26}Mg excesses that imply $(^{26}Al/^{27}Al)_0$ values $\sim 1 \times 10^{-5}$, with some significant spread in this peak of the distribution (Russell *et al.*, 1996; Kita *et al.*, 2000; McKeegan *et al.*, 2000b; Huss *et al.*, 2001; Mostefaoui *et al.*, 2002; Hsu *et al.*, 2003; Kunihiro *et al.*, 2004; Hutcheon and Hutchison, 1989). A couple

of chondrules have $(^{26}Al/^{27}Al)_0$ values that approach the range seen in some CAIs, and Galy *et al.* (2000) report one chondrule (not plotted in Figure 3b) with $(^{26}Al/^{27}Al)_0 = (3.7 \pm 1.2) \times 10^{-5}$, which overlaps the canonical CAI value within uncertainty. Bizzarro *et al.* (2005) reported that ^{26}Al–^{26}Mg model ages for a number of whole chondrules from the Allende CV chondrites covered a range corresponding to 0–1 Myr after the new initial CAI $^{26}Al/^{27}Al$ value. These data are for ICPMS measurement of whole chondrules, and there are currently no data showing internal Al–Mg isochrons for chondrules that fall within error of the CAI value. The overall data imply that chondrule formation began ~1 Myr after the formation of most CAIs and then continued for another ~2 Myr or more. Some chondrules may have formed later still, or, more likely, only achieved closure temperatures for magnesium diffusion following parent-body cooling at times exceeding ~4 Myr after CAIs. That mild metamorphism in chondrites could delay isotopic closure of the Al–Mg system is further evidenced by analyses of plagioclase grains from the H4 chondrites Ste. Marguerite and Forest Vale (Zinner and Göpel, 2002). The inferred $^{26}Al/^{27}Al$ ratios indicate retention of $^{26}Mg^*$ by ~5–6 Myr following CAIs, which is consistent with timescales of parent-body metamorphism implied by absolute Pb–Pb ages of (secondary) phosphates in these meteorites.

A similar temporal interpretation is generally not invoked for those CAIs that exhibit an apparent lack of initial ^{26}Al (Figure 3a). As pointed out by MacPherson *et al.* (1995), many of the inclusions in the low $(^{26}Al/^{27}Al)_0$ peak are not mineralogically altered, which argues against late metamorphism. Moreover, these inclusions are typically hosts for very significant isotopic anomalies in a variety of elements, which argues strongly for their antiquity. Included in this group are the so-called FUN (fractionated and unknown nuclear isotopic effects) inclusions (e.g., Lee *et al.*, 1977, 1980) and the platelet hibonite crystals, which are extremely refractory grains from CM chondrites that are characterized by huge isotopic anomalies in the subiron group elements like titanium and calcium (Fahey *et al.*, 1987; Ireland, 1988). Because of their preservation of extreme stable isotope anomalies, these refractory phases are best understood as having formed at an early time in the nebula, but from an isotopic reservoir (or precursor minerals) that was missing the ^{26}Al inventory sampled by other "normal" refractory materials. The scope of this heterogeneity, both spatially and temporally, is the focus of much conjecture and research, as this is a key issue for the utility of ^{26}Al as a high-resolution chronometer for nebular events (see discussion in Section 1.16.6).

Relatively few data exist for the former presence of ^{26}Al in differentiated (i.e., melted) meteorites, even though there is a widespread assumption that ^{26}Al provided a significant, if not the dominant, heat source for melting of early accreted planetesimals (e.g., Grimm and McSween, 1994; Schramm *et al.*, 1970). Plagioclase crystals in the eucrite Piplia Kalan have significant excess ^{26}Mg (Srinivasan *et al.*, 1999); however, the correlation of $^{26}Mg^*$ with Al/Mg in the plagioclase is poor, indicating that the system has suffered partial reequilibration of magnesium isotopes following crystallization. A best-fit correlation through plagioclase and pyroxene yields an apparent $(^{26}Al/^{27}Al)_0 = (7.5 \pm 0.9) \times 10^{-7}$, which would correspond to ~4 Myr after the CAI canonical value.

Recently, several abstracts have reported Al–Mg data for achondrites, which can potentially be tied to the ^{53}Mn–^{53}Cr system. The petrographically unique eucrite Asuka 881394 exhibits a good Al–Mg isochron with well-resolved $^{26}Mg^*$ in its anorthitic plagioclase that yields $^{26}Al/^{27}Al = (1.19 \pm 0.13) \times 10^{-6}$, corresponding to ~4 Myr after CAIs (Nyquist *et al.*, 2001b). In contrast, the eucrite Juvinas shows only an upper limit of $^{26}Al/^{27}Al \sim 10^{-7}$ (Wadhwa *et al.*, 2003). Basaltic clasts in the ultramafic ureilite DaG-319 all lie on a single Al–Mg isochron with slope $^{26}Al/^{27}Al = (3.95 \pm 0.59) \times 10^{-7}$ indicating that they achieved isotopic closure ~5 Myr after CAI formation (Kita *et al.*, 2003). The data for two angrites (Nyquist *et al.*, 2003) yield a two-point isochron with somewhat lower slope, corresponding to $^{26}Al/^{27}Al = (2.3 \pm 0.8) \times 10^{-7}$. Wadhwa *et al.* (2005) have tied together the Al–Mg, Mn–Cr, and Pb–Pb chronometers for the eucrite Asuka 881394, which has internal isochrons corresponding to $^{26}Al/^{27}Al = (1.34 \pm 0.05) \times 10^{-6}$, $^{53}Mn/^{55}Mn = (4.02 \pm 0.26) \times 10^{-6}$, and an absolute Pb–Pb age of 4.56503 ± 0.00085 Ga. We will return to the interpretation of these data later.

1.16.4.5 Iron-60

^{60}Fe β-decays to ^{60}Ni with a half-life of 1.5 Myr. Unlike the other short-lived nuclides with half-lives of a few million years or less, and in particular contrast to ^{10}Be, ^{60}Fe is not produced by spallation because there are no suitable target elements, and therefore all of its solar system inventory must reflect recent stellar nucleosynthesis. The first plausible evidence for the existence of ^{60}Fe in the solar system was

provided by ^{60}Ni excesses found in bulk samples of the eucrites Chervony Kut and Juvinas (Shukolyukov and Lugmair, 1993a, b). These are basaltic achondrites, the result of planetary-scale melting and differentiation (possibly on the asteroid Vesta; see Chapter 1.11) that fractionated nickel into the core. Thus, the excess ^{60}Ni cannot represent nucleogenetic isotope anomalies of the iron-group elements, as is seen in CAIs, and its presence in such a large volume material indicates wide-scale occurrence of ^{60}Fe in the solar system (Shukolyukov and Lugmair, 1993a). However, internal mineral isochrons could not be obtained on the eucrite samples because of element redistribution after the decay of ^{60}Fe (Shukolyukov and Lugmair, 1993b). Moreover, the inferred initial ^{60}Fe/^{56}Fe differs by an order of magnitude between these eucrites for which other isotopic systems (e.g., ^{53}Mn–^{53}Cr) indicate a similar formation age (Lugmair and Shukolyukov, 1998). These inconsistencies point out problems with interpreting eucrite ^{60}Fe/^{56}Fe abundances in chronologic terms and indicate that estimates of a solar system initial ^{60}Fe/^{56}Fe, based on an absolute age of eucrite formation, is likely subject to large systematic uncertainties.

Recent *in situ* measurements on high Fe/Ni phases in chondrites help to constrain this initial value. Tachibana and Huss (2003) found good correlations of excess ^{60}Ni with Fe/Ni ratios in sulfide minerals of the (LL3.1) unequilibrated ordinary chondrites Bishunpur and Krymka (Figure 6), which imply ^{60}Fe/^{56}Fe ratios of between 1.0×10^{-7} and 1.8×10^{-7}. Mostefaoui *et al.* (2005) reported similar good correlations in troilite from Semarkona (LL3.0) with a slope corresponding to $^{60}\text{Fe}/^{56}\text{Fe} = (9.2 \pm 2.4) \times 10^{-7}$; a weighted regression through their data excluding data points they discounted gives $^{60}\text{Fe}/^{56}\text{Fe} = (9.5 \pm 1.3) \times 10^{-7}$ (Figure 6). They also measured nickel isotopes in magnetite and found a correlation implying $^{60}\text{Fe}/^{56}\text{Fe} = (1.1 \pm 0.4) \times 10^{-7}$. If the two correlations found by Mostefaoui *et al.* (2005) are isochrons, magnetite is ~5 Myr younger than troilite. Although it is somewhat ambiguous whether sulfides achieved isotopic closure in the solar nebula or on an asteroidal parent body, it is likely that they have suffered significantly less disturbance of their Fe–Ni isotopic system than have eucrites, making an extrapolation back to the time of CAI formation more robust. With plausible assumptions, Tachibana and Huss (2003) estimate $(^{60}\text{Fe}/^{56}\text{Fe})_0$ for solar system formation between 1×10^{-7} and 6×10^{-7} with a probable value (depending on the age of the sulfides relative to CAIs) of $(\sim 3\text{–}4) \times 10^{-7}$. Mostefaoui *et al.* (2005) preferred to simply consider their measured ^{60}Fe/^{56}Fe value of 9.2×10^{-7} as a lower limit to the solar system initial value. Further progress has come with the measurement by Tachibana *et al.* (2006) of nickel isotopes in ferromagnesian silicates in chondrules in Semarkona and Bishunpur. They found correlations of excess ^{60}Ni with Fe/Ni ratio consistent with $^{60}\text{Fe}/^{56}\text{Fe} = (2\text{–}3.7) \times 10^{-7}$

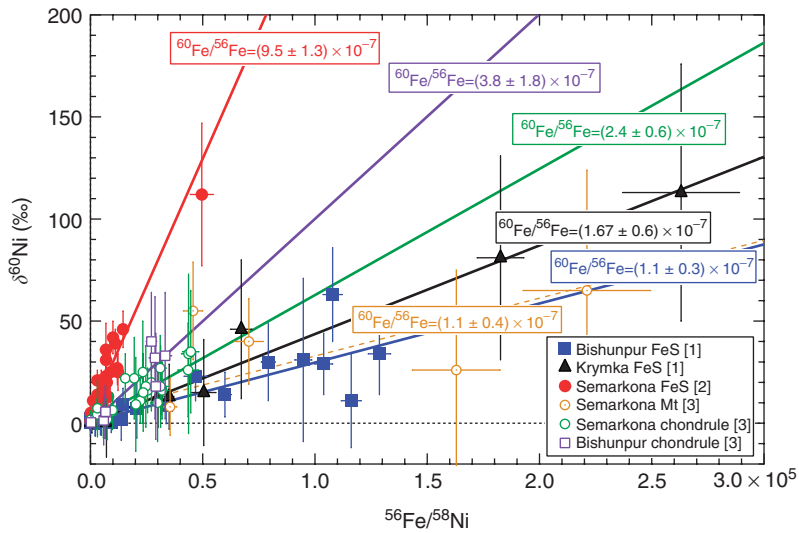

Figure 6 ^{60}Fe–^{60}Ni isochron diagram showing all chondrite data at this writing. Data for all chondrules, all troilite, or all magnetite grains in each meteorite have been grouped and weighted regressions calculated. There is a range of nearly a factor of 10 among the different isochrons, implying a time difference of ~5 Myr among formation ages of these various objects. References: [1] Tachibana and Huss (2003); [2] Mostefaoui *et al.* (2005); [3] Tachibana *et al.* (2006).

(Figure 6). Since ^{26}Al–^{26}Mg chronometry indicates that these chondrules are 1.5–2 Myr older than CAIs, they estimated an initial solar system $^{60}Fe/^{56}Fe$ ratio of (5–10) $\times 10^{-7}$. These data are consistent with an upper limit of $(^{60}Fe/^{56}Fe)_0 = \sim 3.5 \times 10^{-7}$ derived from the analyses of nickel isotopes in FeO-rich olivine from a (LL3.0) Semarkona chondrule which exhibited $(^{26}Al/^{27}Al)_0 = 0.9 \times 10^{-5}$ (Kita *et al.*, 2000). The early solar system estimate of Tachibana *et al.* (2006) is significantly lower than a value of $(^{60}Fe/^{56}Fe)_0 = (1.6 \pm 0.5) \times 10^{-6}$ inferred for an Allende CAI (Birck and Lugmair, 1988), indicating that the ^{60}Ni excesses in this CAI are probably of a nucleosynthetic origin and are not due to *in situ* decay of ^{60}Fe. It would be desirable to have a direct measure of a $^{60}Fe/^{56}Fe$ isochron in a CAI; however, as a volatile element, iron is generally depleted in refractory inclusions and samples containing appropriate mineralogy for this determination may not be found.

The ^{60}Fe–^{60}Ni system is beginning to be applied to differentiated meteorites again, more than 10 years after the pioneering work of Shukolyukov and Lugmair (1993a, b). Moynier *et al.* (2005) reported a correlation for iron meteorites corresponding to a remarkably high $^{60}Fe/^{56}Fe$ value of $(3.0 \pm 0.2) \times 10^{-6}$, but Cook *et al.* (2005, 2006) found no correlation between Fe/Ni and $^{60}Ni/^{58}Ni$ and ^{60}Ni excesses in some of the same samples. Cook *et al.* (2006) reported $^{60}Fe/^{56}Fe = (5.4 \pm 4.2) \times 10^{-7}$, which they did not take as evidence for live ^{60}Fe at the time iron meteorites formed. Bizzarro *et al.* (2006) also performed high-precision MC-ICPMS measurements of nickel isotopes in iron meteorites, finding small deficits of 0.02–0.03‰ in $\delta^{60}Ni$. Using Fe/Ni ratios calculated for initial liquid core compositions, they derive model initial $^{60}Fe/^{56}Fe$ ratios of $(1.48 \pm 0.87) \times 10^{-6}$ and $(1.09 \pm 0.14) \times 10^{-7}$ for IIAB and IIIAB iron meteorites, respectively. If $^{60}Fe/^{56}Fe$ was $\sim 1 \times 10^{-6}$ at the time of CAI formation, this implies core formation before CAI formation, perhaps by as much as 1 Myr. However, Bizzarro *et al.* (2006) also found that the iron meteorites they studied exhibited deficits in $\delta^{62}Ni$, which raises the question of whether the small $\delta^{60}Ni$ deficits could be nucleosynthetic in origin. All of this work is preliminary, but it is clear that further nickel isotopic studies of differentiated meteorites will yield interesting results. The interpretation, however, will require that our understanding of issues of accuracy and isotopic homogeneity of solar system reservoirs advance to a level commensurate with the precision offered by the new analytical methods.

1.16.4.6 Beryllium-10

^{10}Be β-decays to ^{10}B with a half-life of 1.51 Myr. Evidence for its former existence in the solar system is provided by excesses of $^{10}B/^{11}B$ correlated with Be/B ratio (Figure 7), first found within coarse-grained (type B) CAIs from Allende (McKeegan *et al.*, 2000a). From the slope of the correlation line, McKeegan *et al.* calculated an initial $^{10}Be/^{9}Be = (9.5 \pm 1.9) \times 10^{-4}$ at the time corresponding to isotopic closure of the Be–B system. This discovery was rapidly confirmed and extended by analyses of a variety of CAIs of types A and B, and a FUN inclusion from various CV3 chondrites, including Allende, Efremovka, Vigarano, Leoville, and Axtell (MacPherson and Huss, 2001; McKeegan *et al.*, 2001; Sugiura *et al.*, 2001; Chaussidon *et al.*, 2003; MacPherson *et al.*, 2003). The most robust Be–B isochron is that of the Allende CAI 3529-41 (Chaussidon *et al.*, 2006), which is based on 66 ion microprobe spot analyses. Chaussidon *et al.* (2006) reported a slope corresponding to $^{10}Be/^{9}Be = (8.8 \pm 0.6) \times 10^{-4}$, but in their regression, they did not weight data points by their uncertainties. A weighted fit yields $^{10}Be/^{9}Be = (1.038 \pm 0.092) \times 10^{-3}$, which makes this the highest precisely determined initial $^{10}Be/^{9}Be$ ratio found so

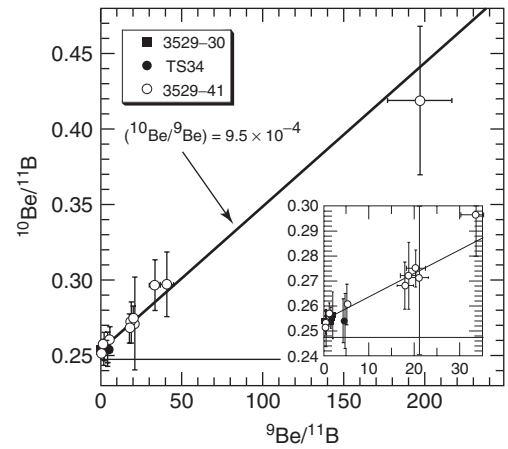

Figure 7 Boron isotopic composition of individual minerals from Allende CAIs as a function of Be/B ratio in the same material; error bars are 2σ. The $^{10}B/^{11}B$ values from various spots of CAI 3529-41 show ^{10}B excesses that are correlated with the Be/B ratio in a manner indicative of the *in situ* decay of ^{10}Be. The slope of the correlation line corresponds to an initial $^{10}Be/^{9}Be = (9.5 \pm 1.9) \times 10^{-4}$ at the time of crystallization. The intercept indicates $^{10}B/^{11}B = 0.254 \pm 0.002$, which is higher than $^{10}B/^{11}B$ for CI chondrites (shown by the horizontal line). Inset figure shows the same data at an expanded scale; data for CAIs 3529-30 and TS-34 are consistent with the Be–B isotope systematics of 3529-41. Data and figure reproduced from McKeegan *et al.* (2000a).

far. Of the nearly two dozen CAIs that have been examined so far, in every case for which high Be/B ratios could be found in a sample (i.e., except where boron contamination is prevalent), excesses of $^{10}B/^{11}B$ are measured, implying that the existence of live ^{10}Be was rather widespread in the solar nebula, at least at the locale of CAI formation. Some spread in initial $^{10}Be/^{9}Be$ ratios is apparent, but overall it is remarkably uniform, especially considering the difficulties of the measurements and the susceptibility of samples to contamination by trace amounts of boron (cf., Chaussidon *et al.*, 1997). Calculated initial $^{10}Be/^{9}Be$ ratios for "normal" CV CAIs range only over a factor of 2 from $(\sim 4.5–10.0) \times 10^{-4}$, with no difference seen between type B CAIs (mean of 12 samples: $^{10}Be/^{9}Be = (6.3 \pm 0.4) \times 10^{-4}$) and type A CAIs (mean of five samples: $^{10}Be/^{9}Be = (6.7 \pm 0.6) \times 10^{-4}$). The one FUN inclusion measured, a type A from Axtell (MacPherson *et al.*, 2003), has the lowest initial $^{10}Be/^{9}Be = (3.6 \pm 0.9) \times 10^{-4}$, but even this value is within error of the lower values measured on "normal" (i.e., non-FUN) CAIs. One CAI, Efremovka E44, has been measured independently in two laboratories with excellent agreement (McKeegan *et al.*, 2001; Sugiura *et al.*, 2001), indicating that potential systematic uncertainties are not significant compared with statistical errors. The initial boron isotopic composition (prior to any ^{10}Be decay) is the same among these various CAIs, with a small degree of relative scatter. However, the mean value, $^{10}B/^{11}B = 0.250 \pm 0.001$, is distinct from a chondritic value ($= 0.248$) measured for CI chondrites (Zhai *et al.*, 1996).

The former presence of ^{10}Be was extended to another important class of refractory objects, hibonite from the CM2 Murchison meteorite (Marhas *et al.*, 2002). Hibonite [$CaAl_{12-2x}(Mg_xTi_x)O_{19}$] is one of the most refractory minerals calculated to condense from a gas of solar composition, and is known to host numerous isotopic anomalies, especially in the heavy isotopes of calcium and titanium (Ireland *et al.*, 1985; Zinner *et al.*, 1986; Fahey *et al.*, 1987). Curiously, when these anomalies are of an exceptionally large magnitude (in the ~several to 10% range), the hibonite grains show a distinct lack of evidence for having formed with ^{26}Al (e.g., Ireland, 1988, 1990) or ^{41}Ca (Sahijpal *et al.*, 1998, 2000). Marhas *et al.* (2002) found excesses of $^{10}B/^{11}B$ in three such hibonite grains that are each devoid of either $^{26}Mg^*$ or $^{41}K^*$ from the decay of ^{26}Al and ^{41}Ca, respectively. Collectively, the Be–B data imply $^{10}Be/^{9}Be = (5.2 \pm 2.8) \times 10^{-4}$ when these hibonites formed. This initial $^{10}Be/^{9}Be$ is in the same range as for other refractory inclusions and indicates that existence of ^{10}Be is decoupled from the other two short-lived nuclides that partition into refractory objects, namely ^{26}Al and ^{41}Ca. Even more striking evidence for decoupling of the ^{26}Al–^{26}Mg and ^{10}Be–^{10}B systems came with the report of Marhas and Goswami (2003) that hibonite in the well-known FUN CAI HAL had an initial $^{10}Be/^{9}Be$ ratio in the same range as other CAIs, yet had an initial $^{26}Al/^{27}Al$ ratio three orders of magnitude lower than the canonical early solar system ratio. The significance of this lack of correlation, for both chronology and source of radionuclides, is discussed further below.

Convincing evidence of live ^{10}Be has so far only been found in refractory inclusions because these samples exhibit large volatility-controlled Be–B fractionation. A tantalizing hint for ^{10}Be was found in one anorthite-rich chondrule from a highly unequilibrated (CO3) chondrite: the Be–B correlation diagram displays a large amount of scatter, but an initial $^{10}Be/^{9}Be$ ratio of $7.2 \pm 2.9 \times 10^{-4}$ may be calculated (Sugiura, 2001). This value is similar to that seen in CAIs, but needs to be confirmed by further measurements.

1.16.4.7 Manganese-53

^{53}Mn decays by electron capture to ^{53}Cr with a half-life of 3.7 Myr. This relatively long half-life, and the fact that manganese and chromium are reasonably abundant elements that undergo relative fractionation in evaporation/condensation processes as well as magmatic processes, make the ^{53}Mn–^{53}Cr system particularly interesting for bridging the time period from nebular events to accretion and differentiation of early-formed planetesimals. Accordingly, this system has been intensively investigated and evidence of live ^{53}Mn has now been found in nebular components such as (1) CAIs (Birck and Allègre, 1985, 1988; Papanastassiou *et al.*, 2002) and (2) chondrules (Nyquist *et al.*, 2001a), as well as (3) bulk ordinary chondrites (Nyquist *et al.*, 2001a; Lugmair and Shukolyukov, 1998), (4) bulk carbonaceous chondrites (Birck *et al.*, 1999), (5) CI carbonates (Endress *et al.*, 1996; Hutcheon and Phinney, 1996; Hutcheon *et al.*, 1999b), (6) enstatite chondrite sulfides (Wadhwa *et al.*, 1997), and (7) various achondrites including angrites, eucrites, diogenites, pallasites, and SNC meteorites (Lugmair and Shukolyukov, 1998; Nyquist *et al.*, 2001b, 2003). Owing to the wealth of high-quality data, an impressively detailed high-resolution relative chronometry can be developed (e.g., Lugmair and Shukolyukov, 2001), however

interpretation of the ^{53}Mn–^{53}Cr system with respect to other chronometers is complex, particularly with respect to nebular events. The primary reasons for these complexities are difficulty in evaluating the initial $^{53}Mn/^{55}Mn$ of the solar system and in establishing its homogeneity in the nebula (see discussions in Birck *et al.*, 1999; Lugmair and Shukolyukov, 2001; and Nyquist *et al.*, 2001a).

As with ^{26}Al, ^{41}Ca, and ^{10}Be, the obvious samples in which to try to establish the solar system initial value for $^{53}Mn/^{55}Mn$ are CAIs. However, in this case there are three factors which work against this goal: (1) volatility-controlled fractionation is not favorable when the parent (^{53}Mn) is more volatile than the daughter (^{53}Cr); (2) both manganese and chromium are moderately volatile elements and significantly depleted in CAIs; and (3) the daughter element is known to exhibit nucleogenetic anomalies in most CAIs (e.g., Papanastassiou, 1986). Together, these properties mean that there are no mineral phases with large Mn/Cr in CAIs, and it is not feasible to find large ^{53}Cr excesses that are uniquely and fully attributable to ^{53}Mn decay. Birck and Allègre (1988) first demonstrated the *in situ* decay of ^{53}Mn by correlating ^{53}Cr excesses with Mn/Cr in mineral separates of an Allende inclusion, deriving an initial $^{53}Mn/^{55}Mn = (3.7 \pm 1.2) \times 10^{-5}$. Comparison with other Allende CAIs led these authors to estimate $\sim 4.4 \times 10^{-5}$ as the best initial $^{53}Mn/^{55}Mn$ for CAIs; however, Nyquist *et al.* (2001a) prefer a somewhat lower value $(2.8 \pm 0.3) \times 10^{-5}$ based on the same mineral separate analyses plus consideration of nonradiogenic chromium in a spinel separate from an Efremovka CAI. In recent work, Birck *et al.* (1999) have emphasized that refractory inclusions are inconsistent with the solar system evolution of the ^{53}Mn–^{53}Cr system, noting that the inferred chronology is necessarily model-dependent. Lugmair and Shukolyukov (1998) reach a similar assessment, describing the "chronological meaning of $^{53}Mn/^{55}Mn$ ratios in CAIs" as "tentative." Papanastassiou *et al.* (2002) also studied Mn–Cr systematics of CAIs and concluded that although spinel preserved the initial $^{53}Cr/^{52}Cr$ ratio, manganese with live ^{53}Mn was introduced during secondary alteration, so it was not clear what event was being dated in CAIs.

Whole chondrule Mn–Cr isochrons (Figure 8) have been reported for the ordinary chondrites Chainpur (LL3.4) and Bishunpur (LL3.1) by Nyquist *et al.* (2001a). The chondrules from both meteorites are consistent with a single isochron with $(^{53}Mn/^{55}Mn)_0 = (8.8 \pm 1.9) \times 10^{-6}$ and an intercept $\varepsilon(^{53}Cr) = -0.03 \pm 0.06$ (Figure 5). If the chondrule data are considered with Mn–Cr data for whole chondrites (Nyquist *et al.*, 2001a), then the slope increases slightly to $(^{53}Mn/^{55}Mn)_0 = (9.5 \pm 1.7) \times 10^{-6}$, which Nyquist and colleagues interpret as reflecting the time of Mn/Cr fractionation during the condensation of chondrule precursors. If this occurred in the same nebular environments as CAI mineral condensation characterized by the preferred $(^{53}Mn/^{55}Mn)_0 = 2.8 \times 10^{-5}$, this implies a time difference of 5.8 ± 2.7 Myr. This is significantly longer than the CAI-chondrule timescale inferred from $^{26}Al/^{27}Al$ (also for Bishunpur chondrules); however, it is not clear that the two chronometers are dating the same events (see discussion in Nyquist *et al.*, 2001a).

A more straightforward interpretation of Mn–Cr ages can, in principle, be achieved for planetary differentiates since these certainly homogenized chromium isotopes during melting and also likely underwent Mn/Cr fractionation at a well-defined nebular locale (the asteroid belt). Although Lugmair and Shukolyukov (1998) have argued for heterogeneity of $^{53}Mn/^{55}Mn$ as a function of heliocentric distance, such effects would be negligible considered over the probable distances of formation for the asteroids (meteorite parent bodies). The rapidly cooled angrites provide the anchor point between ^{53}Mn–^{53}Cr and the absolute age determined by Pb–Pb since both isotopic systems should have closed contemporaneously (Lugmair and Shukolyukov, 1998). The olivine fraction of LEW has a high Mn/Cr and thus provides a good precision for the isochron, with $^{53}Mn/^{55}Mn = (1.25 \pm 0.07) \times 10^{-6}$ and $\varepsilon(^{53}Cr) = +0.40 \pm 0.16$ (Lugmair and Shukolyukov, 1998), which is tied to the Pb–Pb age of $4{,}557.8 \pm 0.5$ Ma (Lugmair and Galer, 1992).

As alluded to above in the discussion of absolute ages of differentiated objects, the eucrites have suffered a more prolonged and complex thermal and shock history, which is reflected in their internal ^{53}Mn–^{53}Cr systematics. Despite this, excesses of ^{53}Cr in bulk samples of eucrites are well correlated with Mn/Cr (Figure 8) indicating large-scale differentiation on the eucrite parent body prior to the decay of ^{53}Mn (Lugmair and Shukolyukov, 1998). The slope of the correlation line yields $^{53}Mn/^{55}Mn = (4.7 \pm 0.5) \times 10^{-6}$, which is nearly two half-lives of ^{53}Mn steeper (older) than the 1.25×10^{-6} value obtained for angrites. Thus, these data indicate that the parent asteroid of the eucrites (Vesta?) was totally molten, probably during mantle–core differentiation, at 7.1 ± 0.8 Ma prior to the crystallization of angrite LEW. By calibration with the absolute Pb–Pb chronology of angrites, this indicates

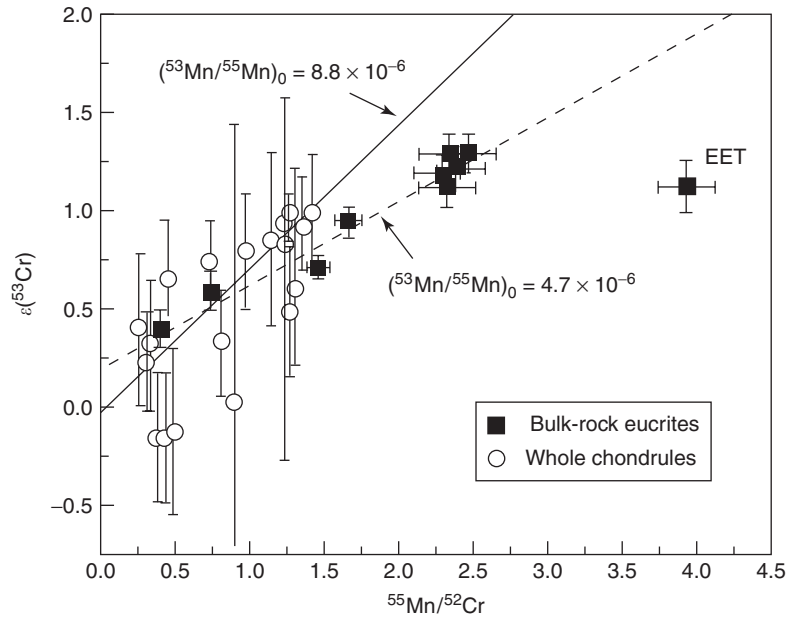

Figure 8 ^{53}Mn–^{53}Cr evolution diagram for nebular components (whole chondrules from ordinary chondrites Bishunpur and Chainpur; Nyquist *et al.*, 2001) and for planetary differentiates (whole-rock eucrites; Lugmair and Shukolyukov, 1998). Plotted are measured values of $\varepsilon(^{53}Cr)$, the deviation of $^{53}Cr/^{52}Cr$ in a sample from the terrestrial standard value in parts per 10^4, as a function of $^{55}Mn/^{52}Cr$. The correlation is interpreted as an isochron indicating the *in situ* decay of ^{53}Mn; the slope for the eucrites (dashed line) corresponds to an initial $^{53}Mn/^{55}Mn = (4.7 \pm 0.5) \times 10^{-6}$ and that for chondrules (solid line) indicates $(^{53}Mn/^{55}Mn)_0 = (8.8 \pm 1.9) \times 10^{-6}$, implying that Mn/Cr fractionation in chondrule precursors preceded global fractionation of the eucrite parent body by approximately one half-life, or ~ 3.5 Myr. All data are replotted from Lugmair and Shukolyukov (1998) and Nyquist *et al.* (2001a); 2σ error bars are indicated and the datum for EET87520 is excluded from the fit for the eucrite whole-rock isochron.

igneous differentiation of the eucrite parent body at $4{,}564.8 \pm 0.9$ Ma (Lugmair and Shukolyukov, 1998). It should be clear that this time does not necessarily represent the crystallization age of individual eucrite meteorites, but the last time of global chromium isotope equilibration and Mn/Cr fractionation. In fact, internal ^{53}Mn–^{53}Cr isochrons for individual cumulate and noncumulate eucrites show a range of apparent $^{53}Mn/^{55}Mn$ values, from close to the global fractionation event (e.g., 3.7×10^{-6} for Chervony Kut) to essentially "dead" ^{53}Mn (e.g., Caldera; Wadhwa and Lugmair, 1996). It is not certain whether these ages, especially the young ones, reflect prolonged igneous activity over a period of tens of millions of years, or cooling ages, or disturbance of the Mn–Cr system by impacts, or some combination of the above (Lugmair and Shukolyukov, 1998). The ^{53}Mn–^{53}Cr ages for individual eucrites do not correlate particularly well with Pb–Pb ages, for example, Chervony Kut with an $^{53}Mn/^{55}Mn$ initial ratio indicating isotopic closure at $\sim 4{,}564$ Ma (almost contemporaneous with mantle differentiation) has a Pb–Pb age of $4{,}312.6 \pm 1.6$ Ma (Galer and Lugmair, 1996). This discrepancy can be attributed to the U–Pb system being more easily disturbed than Mn–Cr (Lugmair and Shukolyukov, 1998); however, as discussed in more detail by Tera and Carlson (1999), it also means that the eucrites cannot serve as an independent check on the validity of coupling ^{53}Mn–^{53}Cr model ages to an absolute timescale based on the Pb–Pb ages of angrites.

Chromium has four stable isotopes, ^{50}Cr, ^{52}Cr, ^{53}Cr, and ^{54}Cr. Mass fractionation in isotopic measurements can alter $^{53}Cr/^{52}Cr$ ratios, but these are corrected by normalizing measured data for all isotopes to the terrestrial $^{50}Cr/^{52}Cr$ ratio. Under the assumption that there are no nucleosynthetic anomalies in ^{54}Cr, Lugmair and colleagues routinely use the small deviations in the mass fractionation-corrected $^{54}Cr/^{52}Cr$ ratio to make a "second-order" correction on $^{53}Cr/^{52}Cr$ (e.g., Lugmair and Shukolyukov, 1998). It has been known for some time that CI and CM chondrites have nucleosynthetic ^{54}Cr anomalies (Rotaru *et al.*, 1992; Podosek *et al.*, 1997). This was recognized for carbonaceous chondrites and ^{54}Cr anomalies were even recognized at the Cretaceous-Tertiary boundary (Shukolyukov and Lugmair, 1998). Trinquier *et al.* (2005a, b) have recently

analyzed a number of meteorites, correcting chromium isotopic data only for mass fractionation using $^{50}Cr/^{52}Cr$ and found that eucrites, diogenites, mesosiderites, and pallasites have a uniform deficit in ^{54}Cr of 0.73 ± 0.02 ε units (parts in 10^4) and that carbonaceous chondrites are enriched in ^{54}Cr by 0.6–1.5ε. Trinquier *et al.* (2005b) reported a new ^{53}Mn–^{53}Cr isochron for basaltic achondrites without making a second-order correction. Their slope corresponded to $^{53}Mn/^{55}Mn = (4.53 \pm 0.17) \times 10^{-5}$, in excellent agreement with Lugmair and Shukolyukov (1998), but the intercept was at $\varepsilon^{53}Cr = -0.15 \pm 0.06$, rather than $+0.25$, a shift of 0.4ε. Lugmair and Shukolyukov (1998) had asserted that a range in intercepts implied a radial gradient in $^{53}Mn/^{55}Mn$ in the early solar system, but the new data of Trinquier *et al.* (2005a, b) are consistent with $^{53}Mn/^{55}Mn$ being homogeneous in the early solar system.

The ^{53}Mn–^{53}Cr system has also proved useful in constraining the timescales of earliest aqueous activity on the parent bodies of some carbonaceous chondrites by dating Mn/Cr fractionation associated with the formation of aqueously precipitated minerals. Carbonates from the CI chondrites Orgueil and Ivuna show very large ^{53}Cr excesses correlated with Mn/Cr; inferred initial $^{53}Mn/^{55}Mn$ ratios range from 1.42×10^{-6} to 1.99×10^{-6} (Endress *et al.*, 1996). Carbonates from other carbonaceous chondrites show a wider range extending to significantly higher initial $^{53}Mn/^{55}Mn$ ratios: $(6.4 \pm 1.2) \times 10^{-6}$ in CM chondrites Nogoya and Y791198, and $(9.4 \pm 1.6) \times 10^{-6}$ in the unusual carbonaceous chondrite Kaidun (Hutcheon *et al.*, 1999a, b). The latter values are similar to $^{53}Mn/^{55}Mn$ found in ordinary chondrite chondrules (Nyquist *et al.*, 2001a). Fayalite (FeO-rich olivine) from the Mokoia oxidized and aqueously altered CV3 chondrite formed with very high $^{55}Mn/^{52}Cr$ ratios ($>10^4$) and exhibits $^{53}Mn/^{55}Mn = (2.32 \pm 0.18) \times 10^{-6}$ (Hutcheon *et al.*, 1998), similar to CI carbonates and eucrites. Mn–Cr data for fayalite from the Kaba chondrite yields the same $^{53}Mn/^{55}Mn$ within uncertainty (Hua *et al.*, 2002).

1.16.4.8 Palladium-107

^{107}Pd β-decays to ^{107}Ag with a half-life of 6.5 Myr. Evidence for this now-extinct nuclide is found in metallic phases of iron meteorites, since large Pd/Ag fractionations occur during magmatic partitioning of metal (Kelly and Wasserburg, 1978; see also review by Wasserburg, 1985). Kaiser and Wasserburg (1983) demonstrated that a linear correlation exists between excess $^{107}Ag/^{109}Ag$ and Pd/Ag in different fractions of metal and sulfide from the group IIIB iron meteorite Grant and from the isochron inferred an initial $^{107}Pd/^{108}Pd = \sim 1.7 \times 10^{-5}$ at the time of crystallization of this meteorite. Extrapolation back to the time of CAI formation would yield an initial $^{107}Pd/^{108}Pd$ of approximately twice this value for the solar system, though with considerable uncertainty. Further isochrons were determining in other many iron and stony-iron meteorites, showing that there is a wide range of initial $^{107}Pd/^{108}Pd$ ratios, but that many samples have ratios in the range $(1.5–2.5) \times 10^{-5}$ (Chen and Wasserburg, 1996; Chen *et al.*, 2002). Recently, Carlson and Hauri (2001) have developed ICPMS methods for determining silver isotope ratios with high precision, thus permitting the investigation of phases with more moderate Pd/Ag fractionation. They found good isochrons for the pallasite (stony-iron) Brenham and the IIIB iron Grant, both with inferred initial $^{107}Pd/^{108}Pd = 1.6 \times 10^{-5}$. A two-point correlation between metal and sulfide was also determined for Canyon Diablo (group IA iron), yielding an apparent initial $^{107}Pd/^{108}Pd$ essentially identical to that previously found for Gibeon (Chen and Wasserburg, 1990). Interpreted chronologically, the data imply that Brenham and Grant formed some 3.5 Myr following Canyon Diablo and Gibeon. Small (5ε) $^{107}Ag/^{109}Ag$ anomalies were also documented for the carbonaceous chondrite Allende (Carlson and Hauri, 2001), which, given its relatively low Pd/Ag content, would imply an enormous initial $^{107}Pd/^{108}Pd$ ($\sim 39 \times 10^{-5}$) if this anomaly had evolved from the most unradiogenic sample (Canyon Diablo sulfide) due to ^{107}Pd decay only. However, no internal isochron is obtained for Allende and considering its unequilibrated nature (i.e., it hosts many isotopic anomalies) there is no compelling reason to assume that this value represents a solar nebular abundance of live ^{107}Pd.

1.16.4.9 Hafnium-182

^{182}Hf β-decays to ^{182}W with a half-life of 9 Myr. This has been recognized as an extremely important isotopic system in recent years (e.g., Lee and Halliday, 1996; Halliday and Lee, 1999) because it is almost uniquely sensitive to metal–silicate fractionation and its rather long half-life makes it a useful probe for both nebular and planetary processes. Specifically, tungsten is highly siderophile whereas hafnium is retained in silicates during melting and metal segregation. Thus, tungsten isotope compositions could be very different in silicates and metal from distinct planetary objects depending on whether or

not metal/silicate fractionation in those objects predated significant decay of ^{182}Hf. Internal isochrons, demonstrating good correlations of ^{182}W/^{180}W with Hf/W, are found for several separates of ordinary chondrites (Kleine *et al.*, 2002a, b; Yin *et al.*, 2002); samples of whole-rock carbonaceous chondrites and a CAI from Allende also fall within error of these isochrons (Yin *et al.*, 2002). The Pb–Pb ages of phosphates in the ordinary chondrites (Kleine *et al.*, 2002a) and the coincidence of the CAI data (Yin *et al.*, 2002) allow a robust estimate of the initial ^{182}Hf/^{180}Hf of the solar system of 1.0–1.1 $\times 10^{-4}$ with an initial ^{182}W/^{180}W significantly ($\sim -3\varepsilon$) lower than terrestrial mantle samples. A regression through data for two bulk CAIs, several fragments of a single CAI, and bulk carbonaceous chondrites yields the most robust currently available early solar system ^{182}Hf/^{180}Hf value, $(1.07 \pm 0.10) \times 10^{-4}$, and ε^{182}W value, −3.47 (Kleine *et al.*, 2005).

Iron meteorites have ε^{182}W values similar or below the early solar system estimated value of $\varepsilon^{182}\text{W} = -3.47$ (Kleine *et al.*, 2005a; Markowski *et al.*, 2006; Qin *et al.*, 2006). The values below the early solar system value apparently result from cosmic ray exposure effects, but it does appear that a number of iron meteorites have the same tungsten isotopic composition as the early solar system. This implies that metal–silicate segregation occurred no later than 1 Myr after the formation of CAIs (Kleine *et al.*, 2005a; Markowski *et al.*, 2006; Qin *et al.*, 2006). Tungsten isotopes have also been used to show that most eucrites experienced a thermal event 16 ± 2 Myr after mantle–crust differentiation in the eucrite parent body (Kleine *et al.*, 2005b).

The meaning of tungsten isotopes with regard to timescales of accretion and core formation of the Earth and formation of the Moon is discussed in Chapter 1.20. Tungsten isotope constraints on processes on Mars are discussed in Chapter 1.22.

1.16.4.10 Iodine-129

^{129}I β-decays to ^{129}Xe with a half-life of 15.7 Myr. As mentioned in the historical introduction (Section 1.16.1.3), ^{129}I was the first extinct isotope whose presence in the early solar system was inferred from excesses of its daughter ^{129}Xe in meteorites (Jeffery and Reynolds, 1961). Both parent and daughter are mobile elements, and coupled with the relatively long half-life, this means that closure effects on the I–Xe system likely limit its utility to parent-body processes (e.g., Swindle *et al.*, 1996), although arguments have been advanced that I–Xe can date nebular events in favorable circumstances (Whitby *et al.*, 2001). New analytical techniques that enable the investigation of single mineral phases (Gilmour, 2000; Gilmour and Saxton, 2001) have helped in the understanding of apparent I–Xe isochrons (as differentiated from mixing lines of multiple phases) and enabled more confident chronological interpretations, particularly of secondary mineral phases formed on asteroidal parent bodies. Brazzle *et al.* (1999) demonstrated concordancy between I–Xe and Pb–Pb chronometers for chondrite phosphates over a timescale of tens of millions of years. At another extreme, Whitby *et al.* (2000) found an initial ratio of $^{129}\text{I}/^{127}\text{I} = (1.35 \pm 0.05) \times 10^{-4}$ in halite from a relatively unequilibrated ordinary chondrite. This result is close to the estimated initial value for the solar system ($\sim 10^{-4}$), implying that the aqueous activity responsible for precipitating the halite occurred immediately upon accretion, probably within a few million years of CAI formation (Whitby *et al.*, 2000).

1.16.4.11 Lead-205

^{205}Pb decays by electron capture to ^{205}Tl with a half-life of 17.3 Myr. It is unique among the short-lived radionuclides present in the early solar system in being produced only by s-process nucleosynthesis (see Chapter 1.01). Nielsen *et al.* (2006) reported a correlation between ^{205}Tl/^{203}Tl and ^{204}Pb/^{203}Tl ratios among metal and troilite from the IAB iron meteorites Toluca and Canyon Diablo that was consistent with $^{205}\text{Pb}/^{204}\text{Pb} = (7.4 \pm 1.0) \times 10^{-5}$. The range in ^{205}Tl/^{203}Tl is $\sim$5‰ and Nielsen *et al.* (2006) conclude that mixing of mass-fractionated components is unlikely to be the cause of this variation. Nielsen *et al.* (2006) used the I–Xe age of IAB silicate inclusions to calculate an early solar system ^{205}Pb/^{204}Pb value of (1.0–2.1) $\times 10^{-4}$.

1.16.4.12 Niobium-92

^{92}Nb decays by electron capture to ^{92}Zr with a half-life of 36 Ma. ^{92}Nb is a p-process nuclide (see Chapter 1.01). The first hint that this isotope was present in the early solar system was based on an $8.8 \pm 1.7\varepsilon$ excess in ^{92}Zr in a niobium-rich rutile grain from the Toluca IAB iron meteorite (Harper, 1996). This corresponded to an initial ^{92}Nb/^{93}Nb ratio of $(1.6 \pm 0.3) \times 10^{-5}$, but the time of formation of Toluca rutile is not known. Three subsequent studies that used MC-ICPMS to measure zirconium isotopic composition reported that the initial solar system ^{92}Nb/^{93}Nb was $\sim 10^{-3}$, higher by two orders of magnitude

(Yin *et al.*, 2000; Münker *et al.*, 2000; Sanloup *et al.*, 2000). This initial $^{92}Nb/^{93}Nb$ was nearly one quarter of the p-process production ratio (Harper, 1996) and was difficult to understand, as most ^{93}Nb is made by the s-process. The situation was resolved with the work of Schönbachler *et al.* (2002), who reported internal Nb–Zr isochrons for the Estacado H6 chondrite and for a clast from the Vaca Muerta mesosiderite, both of which give an initial solar system $^{92}Nb/^{93}Nb$ of $\sim 10^{-5}$, a much more plausible value in terms of nucleosynthetic considerations. This lower initial ratio limits the utility of the ^{92}Nb–^{92}Zr for chronometry (see Chapter 1.20 for further discussion).

1.16.4.13 Plutonium-244 and Samarium-146

These relatively long-lived isotopes are mentioned here for completeness since both have been shown to have existed in the early solar system. However, neither ^{244}Pu nor ^{146}Sm has been developed for chronological applications, for very practical reasons. ^{244}Pu suffers from the fact that there are no long-lived isotopes of plutonium against which to normalize its abundance, and its primary application in meteorite studies is for obtaining cooling rates from the annealing of fission tracks in appropriate minerals. The half-life of ^{146}Sm (103 Myr) is too long and its abundance and relative fractionation from daughter ^{142}Nd are insufficient for it to constitute a useful chronometer for early solar system processes. Its primary interest is for nuclear astrophysics (e.g., Prinzhofer *et al.*, 1989), because this isotope is on the neutron-deficient side of the valley of β-stability. Interested readers are referred to Stewart *et al.* (1994) and review by Podosek and Swindle (1988) and Wasserburg (1985) for more information.

1.16.5 ORIGINS OF THE SHORT-LIVED NUCLIDES IN THE EARLY SOLAR SYSTEM

The ability of short-lived radioisotopes to function as chronometers for the early solar system is critically dependent on there having been an initially uniform distribution of the radioactivity throughout the nebula, or at least in those regions from which meteoritic components are derived. Only in this circumstance can differences in initial abundances of a radionuclide compared with a stable counterpart, as inferred by the excesses of the respective daughter isotope, be interpreted as due to radioactive decay from the initial inventory. The homogeneity of the distribution of radionuclides in the solar nebula depends, in turn, on the processes that created those isotopes some time before the formation of early solar system materials. For the longer-lived isotopes listed in Table 1 (e.g., ^{182}Hf, ^{129}I, ^{205}Pb, ^{92}Nb, ^{146}Sm, and ^{244}Pu), continuous nucleosynthesis may have been sufficient to produce a quasi-equilibrium abundance of these species that was inherited by the solar nebula. However, the shorter half-life isotopes require a more immediate source (e.g., Meyer and Clayton, 2000; Wasserburg *et al.*, 1996).

In principle, new (radioactive) isotopes could have been created by nuclear processes within the solar nebula itself, or they could have originated from sources external to the nebula. In the latter case, the most likely source is stellar nucleosynthesis in the interiors of nearby mass-losing stars (e.g., Cameron, 2001a, b; Cameron *et al.*, 1995; Wasserburg *et al.*, 1994, 1996, 1998), although spallation reactions in the molecular cloud parental to the solar nebula are also a possibility. If short-lived radioactivity is produced locally, for example, by spallation reactions with nuclear particles (protons and alphas) accelerated by interaction with an active young Sun (e.g., Gounelle *et al.*, 2001; Lee *et al.*, 1998), then it is unlikely that the products of those reactions will be distributed uniformly throughout the accretion disk. Homogeneity over nebular scale-lengths is much more likely for an "external seeding" scenario, although even in this case strong isotopic heterogeneity is possible at the very early stages following injection, before local mixing can act to smooth out the memory of the particular mechanism for "contamination" of the nebula by the new isotopes. The injection of radioactive stellar debris in a "triggered" collapse scenario for solar system formation is reviewed by Boss and Vanhala (2001); later, we consider the possible implications of this model for understanding isotopic heterogeneities in certain refractory inclusions.

The possible stellar sources of the short-lived isotopes, as well as constraints on nuclear spallation processes that could have produced them, are reviewed in detail by Goswami and Vanhala (2000). Since that work, three new developments have occurred: the discovery of evidence for live ^{10}Be in CAIs (McKeegan *et al.*, 2000a); the observation of *in situ* ^{60}Fe decay in chondrites (Tachibana and Huss, 2003; Mostefaoui *et al.*, 2005; Tachibana *et al.*, 2006) that leads to a factor of ~ 20 increase in the estimated $(^{60}Fe/^{56}Fe)_0$ for the solar system initial; and the observation of *in situ* ^{36}Cl decay in secondary alteration phases in CAIs (Lin *et al.*, 2005; Hsu *et al.*, 2006). These

isotopes are particularly significant because their respective modes of origin are much more tightly constrained than those of the other extinct nuclides. ^{10}Be is not produced by stellar nucleosynthesis, thus its existence in the early solar system is strong evidence for a spallogenic source of some short-lived nuclides. The amount of ^{36}Cl inferred for the early solar system is higher than is plausible for stellar sources, implying a late episode of irradiation in the early solar system (Hsu *et al.*, 2006). However, ^{60}Fe is not produced by spallation reactions, but it is produced in core-collapse supernovae and in intermediate mass asymptotic giant branch (AGB) stars (Wasserburg *et al.*, 1994, 2006; Busso *et al.*, 1999). The existence of ^{60}Fe in the relatively high abundance of $(5–10) \times 10^{-7}$ is therefore compelling evidence that stellar debris seeded the early solar system with new radioactivity. A recently proposed hypothesis considers that the source of spallogenic ^{10}Be is actually magnetically trapped cosmic rays in the interstellar medium prior to the collapse of a molecular cloud to form the solar system (Desch *et al.*, 2004). An alternative model considers ^{10}Be to be produced during supernova explosions (Cameron, 2001a, b), but there are problems in coproducing ^{10}Be with other short-lived isotopes (see below). Both modes of origin are doubtful and would be firmly ruled out if the existence of live ^{7}Be in early solar system objects, as suggested by the analyses of an Allende CAI by Chaussidon *et al.* (2006), can be corroborated by Li–Be–B studies of other samples. The abundance of ^{10}Be in CAIs is consistent with expectations based on observations of X-ray luminosity in young, solar-like stars (Feigelson *et al.*, 2002a, b; Preibisch *et al.*, 2005) and models of particle acceleration due to magnetic flare activity near the protosun (Lee *et al.*, 1998; Leya *et al.*, 2003). In summary, the most likely scenario implied by the new meteoritic data is that the overall inventory of extinct nuclides contained both a spallogenic component, probably produced locally, and a nucleogenetic component, probably produced in a supernova, although contributions from AGB and other rapidly evolving mass-losing stars are also possible. Supernovae are often associated with star-forming regions (e.g., Hester *et al.*, 2004; Ouellette *et al.*, 2005), whereas low- and intermediate-mass AGB stars take much longer to evolve and are more or less randomly distributed relative to star-forming regions. Busso *et al.* (1999) and Wasserburg *et al.* (2006) have considered these issues in detail.

Although ^{10}Be and ^{60}Fe are interesting isotopes for delimiting possible origins of short-lived radioactivity, it is ^{41}Ca, ^{26}Al, and ^{53}Mn that are potentially most useful for chronology. Thus, a key task is to sort out, quantitatively, what sources are responsible for these isotopes in the early solar system. This can be addressed theoretically for both stellar and spallogenic sources; however, a clear consensus is lacking (e.g., Goswami *et al.*, 2001; Gounelle *et al.*, 2001; Leya *et al.*, 2003) since production models can be tweaked by adjustable parameters (e.g., energy spectrum and target compositions) that are poorly constrained by observation. Another approach is to examine the isotopic record in meteoritic components for correlations that may indicate common sources (and distributions) for these nuclides.

The refractory inclusions provide the best samples since they incorporated all three of these radioisotopes as well as ^{10}Be. It has already been mentioned that ^{41}Ca and ^{26}Al are highly correlated in CAIs and hibonite grains (Figure 2). At face value, this would imply the same source for both these refractory elements. A problem with ^{41}Ca, however, is that its abundance is only marginally above detection limits and it decays very quickly, so that there is essentially no chance to test for concordant decay between the ^{41}Ca and ^{26}Al systems. This is not the case for ^{26}Al and ^{10}Be, which exist in much higher abundances and which have half-lives that differ by only a factor of 2.

The initial ^{26}Al/^{27}Al and ^{10}Be/^{9}Be values have been measured in a variety of refractory phases from both CV and CM carbonaceous chondrites (Figure 9). ''Normal'' CAIs of both petrologic types A and B have inferred ^{26}Al/^{27}Al values that plot within error of $\sim 5 \times 10^{-5}$ that is typical for CAI crystallization; even for cases where the Al–Mg system is disturbed in anorthite, other phases in the inclusion plot near this value (e.g., Sugiura *et al.*, 2001). As noted above, initial ^{10}Be/^{9}Be ratios for ''normal'' CV CAIs also show no discrimination based on petrology and the total range covered is approximately a factor of 2, which is only marginally outside of experimental uncertainty. Thus, for normal CAIs it is difficult to claim that the two isotopic systems are definitively discordant since the resolution of the data is not quite good enough.

However, the situation is different when one considers hibonites-rich and FUN inclusions (Figure 9). For most of these objects only an upper limit on initial ^{26}Al/^{27}Al ($< \sim 10^{-5}$) is obtained, yet they have initial ^{10}Be/^{9}Be similar to most of the other refractory inclusions (MacPherson *et al.*, 2003; Marhas *et al.*, 2002; Marhas and Goswami, 2003). The data are still not completely convincing until one includes the famous FUN inclusion ''HAL'' (Lee *et al.*,

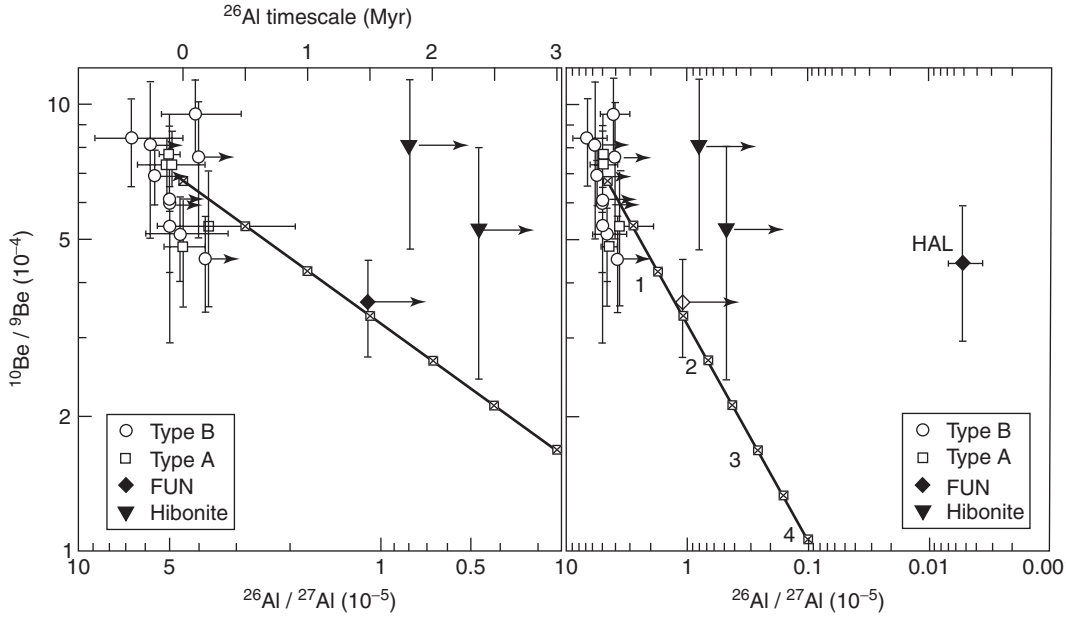

Figure 9 Inferred initial $^{26}Al/^{27}Al$ versus initial $^{10}Be/^{9}Be$ for refractory inclusions in CM and CV carbonaceous chondrites. All data are plotted with 2σ errors; upper limits are indicated by arrows. The locus of concordant ages by free decay from assumed solar system initial values of $^{26}Al/^{27}Al = 4.5 \times 10^{-5}$ and $^{10}Be/^{9}Be = 6.7 \times 10^{-4}$ is shown by the heavy line with 0.5 Myr tick marks. Left panel: the $^{26}Al/^{27}Al$ timescale is also shown on the top axis. It may be seen that "normal" CAIs of both petrologic types A and B have maximal $^{26}Al/^{27}Al$ values that plot within error of the "canonical" solar system initial, but the FUN inclusion (Axtell 2771; MacPherson *et al.*, 2003) and the CM hibonite grains (Marhas *et al.*, 2002) are depleted in ^{26}Al, with upper limits $< \sim 10^{-5}$. For nearly half of the type B CAIs, the Al–Mg system shows evidence of secondary disturbance; in these cases the maximum inferred $^{26}Al/^{27}Al$ is plotted as an upper limit (i.e., the inclusions are assumed to have formed with close to these values). With this approximation, the normal CAIs are relatively tightly clustered in $^{26}Al/^{27}Al$, but show a range of approximately a factor 2 in $^{10}Be/^{9}Be$, which is resolved at the 2σ level for several cases. Right panel: expanded scale showing new data from Marhas and Goswami (2003). In contrast to other FUN inclusions, HAL shows resolved ^{26}Mg excesses (Fahey *et al.*, 1987) implying a very low initial $^{26}Al/^{27}Al = (5.2 \pm 1.7) \times 10^{-8}$, but it also has $^{10}Be/^{9}Be$ similar to other refractory inclusions (Marhas and Goswami, 2003), demonstrating that ^{10}Be and ^{26}Al are decoupled. Data sources: Fahey *et al.* (1987), Podosek *et al.* (1991), McKeegan *et al.* (2000a, 2001), Srinivasan (2001), Sugiura *et al.* (2001), MacPherson *et al.* (2003), Marhas *et al.* (2002), and Marhas and Goswami (2003).

1978, 1980). Recent analyses by Marhas and Goswami (2003) demonstrate that this hibonite-rich Allende CAI has $^{10}B/^{11}B$ excesses that imply $^{10}Be/^{9}Be = \sim 4 \times 10^{-4}$, close to that of other CAIs, yet HAL has a well-resolved, but exceedingly low, initial $^{26}Al/^{27}Al = 5 \times 10^{-8}$ (Fahey *et al.*, 1987). These data clearly demonstrate that HAL formed from a reservoir with a characteristic $^{10}Be/^{9}Be$ similar to that of other refractory materials, but that it was almost completely lacking in $^{26}Al/^{27}Al$. The low value of $^{26}Al/^{27}Al$ that it does have may, in fact, be commensurate with ambient background in the molecular cloud, that is, independent of any specific additional source of ^{26}Al that spiked the CAI-forming regions of the solar nebula (Marhas and Goswami, 2003). Because the ^{10}Be is clearly spallogenic, this provides strong evidence that the vast majority of the ^{26}Al cannot have been produced that way and therefore that essentially all ^{26}Al is derived from external seeding of the nebula. The correlation of ^{26}Al with ^{41}Ca, even though it is not temporally quantitative, is then further evidence for the coproduction and injection of these nuclides into the solar nebula as freshly synthesized stellar debris.

Unfortunately, similar arguments cannot be advanced for ^{53}Mn, primarily because of the poor constraints on initial $^{53}Mn/^{55}Mn$ in CAIs. As discussed further below, the Mn–Cr systematics of nebular components are difficult to interpret in terms of a reasonable chronology, and one possible reason for this could be a significant contribution to the ^{53}Mn inventory by local production processes.

1.16.6 IMPLICATIONS FOR CHRONOLOGY

In principle, the record of each of the now-extinct isotopes can be interpreted to infer a

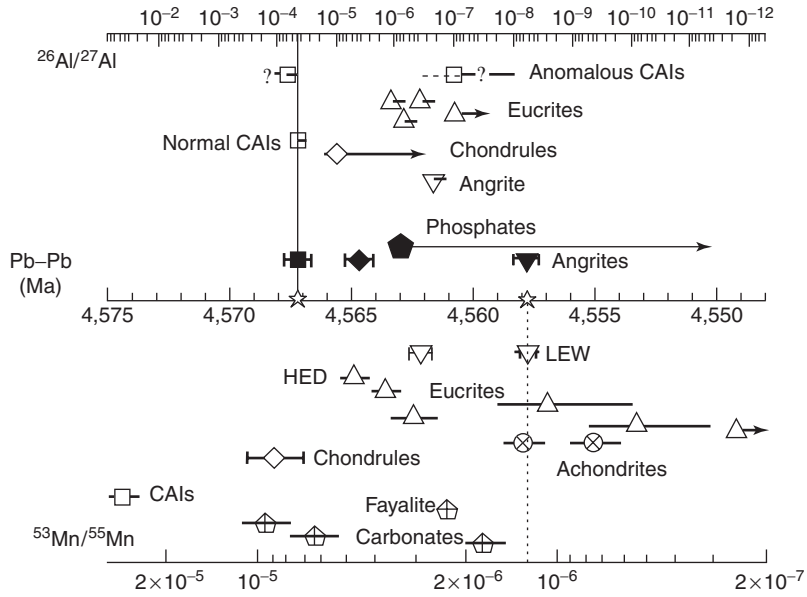

Figure 10 Timeline for early solar system events integrating the ^{26}Al–^{26}Mg and ^{53}Mn–^{53}Cr short-lived chronometers with the absolute timescale provided by the Pb–Pb chronometer. The anchor points (vertical dashed lines) are (1) the Pb–Pb age of CAIs (Amelin *et al.*, 2002) with "canonical" ^{26}Al/^{27}Al and (2) the Pb–Pb age of angrites (Lugmair and Galer, 1992) with the ^{53}Mn/^{55}Mn ratio in LEW (Lugmair and Shukolyukov, 1998). Pb–Pb ages are indicated for the filled symbols read against the absolute timescale (central axis); the top axis shows the initial ^{26}Al/^{27}Al values measured in various phases (open symbols) and the bottom axis refers to initial ^{53}Mn/^{55}Mn for the open symbols in the bottom panel. Squares—CAIs, diamonds—chondrules, upright triangles—eucrites (basaltic achondrites), inverted triangles—angrites, crossed circles—pallasites and Acapulco, and pentagons—secondary minerals in chondrites (phosphates, carbonates, and fayalite). The datum labeled "HED" represents the Mn–Cr correlation line for bulk eucrites. "LEW" refers to the anchor point for ^{53}Mn/^{55}Mn and Pb–Pb; the remaining angrite datum represents Mn–Cr and Al–Mg analyses of D'Orbigny (Nyquist *et al.*, 2003). "Anomalous CAIs" refers to those that apparently formed with no live ^{26}Al—see text for discussion.

chronology for various events that caused chemical fractionations in early solar system materials. Here we evaluate the consistency of these records, both internally and with each other, as well as with the Pb–Pb chronometer, to determine what quantitative constraints can be confidently inferred for the sequence and duration of processes in the solar nebula and on earliest planetesimals (planetary-scale differentiation, for example, relative to the Earth, is considered in Chapter 1.20). To obtain reference points for cross-calibrating relative and absolute chronologies, we require samples which achieved rapid isotopic closure following a well-defined fractionation event and for which a robust and high-precision data set exists. By these criteria, only two anchor points are possible for the cross-calibration: (1) the Pb–Pb and Al–Mg records in CAIs and (2) the Pb–Pb and Mn–Cr records in angrites. As demonstrated in Figure 10, the former provides a reasonably self-consistent, high-resolution record for nebular events, and the latter yields unique temporal information regarding early planetary differentiation processes, but that global consistency between the Al–Mg and Mn–Cr systems is problematic. The existing record for the other short-lived radionuclides is either not well-preserved across different types of samples (e.g., ^{41}Ca, ^{10}Be, and ^{182}Hf), or is insufficiently precise or uncertain as to the nature of isotopic closure (e.g., ^{60}Fe and ^{129}I) so that cross-calibrations spanning the nebular and planetary accretion timescales are not yet possible.

1.16.6.1 Formation Timescales of Nebular Materials

A consistent timescale for fractionation events that occurred during high-temperature processing of nebular materials is obtained (Figure 10) by fixing the canonical ^{26}Al/^{27}Al value (4.5×10^{-5}) measured in CAIs to the absolute timescale provided by the recent high-precision Pb–Pb isochron age of $4{,}567.11\pm0.16$ Ma (Amelin *et al.*, 2006). There is an uncertainty in tying these timescales together here, in that it is not clear whether

the Pb–Pb age of CAIs is the crystallization age, where $^{26}Al/^{27}Al = 4.5 \times 10^{-5}$ would be appropriate, or the time of nebular Al/Mg fractionation, in which case $^{26}Al/^{27}Al = 6.3 \times 10^{-5}$ would be a better choice. These two $^{26}Al/^{27}$Al choices differ in time by 350 kyr. By this calibration, the initial $^{26}Al/^{27}Al$ values inferred for chondrules from the most unequilibrated chondrites ($\sim 1 \times 10^{-5}$; Figure 3) indicate that chondrule formation began by at least $\sim$4,565 Ma and continued probably for another $\sim$1–2 Myr. This time frame fits with a high-precision Pb–Pb isochron for chondrules (from CR chondrites) which yields 4,564.7 $\pm$ 0.6 Ma (Figure 1). Chondrule ages which appear younger than $\sim$4,563 by Al–Mg probably reflect metamorphic cooling rather than nebular formation, still younger Pb–Pb ages may reflect alternative, late formation scenarios, such as protoplanetary collisions (Krot *et al.*, 2005).

The same is not true for the majority of "anomalous CAIs," those that apparently formed lacking any significant live ^{26}Al. These refractory inclusions, which are often hibonite-rich, typically exhibit very large anomalies in "stable" isotopes (e.g., calcium or titanium) that are most readily interpreted as indicating a lack of mixing with average solar nebula materials. Because isotopic homogenization is expected to be an ongoing process during nebular evolution, the preservation of these anomalies argues strongly for a very "primitive" nature of these materials, that is, they probably formed early (not late) and also they escaped any significant isotopic reequilibration from later heating (MacPherson *et al.*, 1995; Sahijpal and Goswami, 1998). Sahijpal and Goswami (1998) suggested that the highly anomalous CM hibonite grains might have formed in a triggered collapse scenario just prior to injection of the radionuclides (^{41}Ca and ^{26}Al), which could theoretically trail the shock front (Foster and Boss, 1997). It would be useful to demonstrate the plausibility of this scenario by measuring an absolute Pb–Pb age on a suite of these objects; even if such a measurement might lack the precision to resolve the prearrival interval, it could at least demonstrate that the samples were not anomalously young.

There are other refractory inclusions, for example, grossite-bearing CAIs from CH chondrites (Weber *et al.*, 1995), which do not fit this model since they lack calcium and titanium isotopic anomalies as well as ^{26}Al. One interpretation of such objects could be that CAI formation lasted several million years, but this is not supported by any independent evidence and there could well be other reasons for the lack of both short-lived radioactivity and large isotopic anomalies (aside from ^{16}O excesses; Sahijpal *et al.*, 1999) in these inclusions. Circumstantial arguments against a long time period for CAI formation are that it leads to problems with understanding the distribution of the oxygen isotope anomalies in nebular components (see Chapters 1.06–1.08; also McKeegan and Leshin, 2001) and with calculations of dynamical lifetimes of CAIs as independent objects in the nebula (Weidenschilling, 1977). Alternative explanations must invoke spatial heterogeneity within the nebula, either with respect to radionuclide distribution or CAI distribution, or both. It is beyond the scope of this review to critically assess models of turbulence and mixing in the solar nebula or evidence regarding the provenance of various CAI types; see Shu *et al.* (2001), Cuzzi *et al.* (2003), McKeegan *et al.* (2000a), Krot *et al.* (2002) and Alexander *et al.* (2001) for discussions.

Difficulties in interpreting an absence of ^{26}Al in some samples notwithstanding, on the basis of the good concordance of the Al–Mg and Pb–Pb systems the first-order conclusion is that $^{26}Al/^{27}Al$ records do have chronological significance for most CAIs and chondrules. Taking the conventional (and reasonable) point of view that chondrules are nebular products, their formation ages relative to normal CAIs imply a duration of at least $\sim$2–3 Myr for the solar nebula. Such a duration is plausible from an astrophysical viewpoint (Podosek and Cassen, 1994; Cameron, 1995), and it has interesting implications for timescales of accretion and radioactive heating of early-formed planetary bodies.

The nebular chronology inferred from initial $^{53}Mn/^{55}Mn$ (Figure 10) is not consistent with the Al–Mg and Pb–Pb systems either in terms of intervals or absolute ages (when Mn–Cr is anchored by the absolute Pb–Pb age of the LEW 86020 angrite, Lugmair and Galer, 1992). Because $(^{53}Mn/^{55}Mn)_0$ is poorly defined for CAIs (see above and discussion in Nyquist *et al.*, 2001a), the inferred interval between CAI and chondrule formation is rather uncertain, but is at least 4 Myr, with a more likely minimum value of $\sim$6 Myr (Nyquist *et al.*, 2001a). The angrite-calibrated $^{53}Mn/^{55}$Mn age of CAIs is too old by a minimum of 7 Myr compared with the measured Pb–Pb age, and chondrules are calculated to be $\sim$1–2 Myr older than their measured Pb–Pb absolute age.

The discrepancies due to aberrantly old Mn–Cr ages of CAIs and chondrules were recognized by Lugmair and Shukolyukov (2001), who argued that a 4,571 Ma absolute age of the solar system, with $(^{53}Mn/^{55}Mn)_0 = 1.4 \times 10^{-5}$, would resolve the difficulties. In this case, $^{53}Mn/^{55}$Mn could not be used to date CAI formation. More

significantly, this would imply that Pb–Pb ages of CAIs could not be crystallization ages but must (based on the time interval) represent metamorphic cooling times. A problem with such an interpretation is the apparently unique composition of initial lead in CAIs (Tera and Carlson, 1999), which could not be maintained in a parent-body setting above the closure temperature for lead diffusion. Additionally, this interpretation (based on a model of chromium isotopic evolution in the solar nebula) runs counter to the good concordance of the Al–Mg system with Pb–Pb. At this time, it seems more reasonable to conclude that Mn–Cr does not provide a consistent high-resolution chronology for nebular events because one or more of the assumptions (initial homogeneity, isotopic closure, etc.) regarding the behavior of this short-lived chronometer is not satisfied within nebular components of chondrites.

A relatively long interval (>4 Myr) between CAIs and chondrules can be inferred on the basis of I–Xe dating (see Swindle *et al.*, 1996 for a review). At face value, this might be seen as support for an Mn–Cr age for chondrule formation; however, in detail it does not work. The siting of ^{129}I is uncertain in both CAIs and chondrules and isotopic closure effects are evidenced by I–Xe apparent ages of chondrules that span an interval of up to several tens of millions of years, implicating asteroidal rather than nebular processes (e.g., Swindle *et al.*, 1991).

1.16.6.2 Timescales of Planetesimal Accretion and Early Chemical Differentiation

Although the interpretation of apparent initial ^{53}Mn/^{55}Mn values in terms of a chronology for nebular fractionation events is problematic, the Mn–Cr system seems amenable to timing chemical fractionations associated with ''geologic'' activity on early-formed planetary bodies. A timescale is presented in the bottom panel of Figure 10, following the suggestion of Lugmair and Shukolyukov (1998) to utilize the LEW86010 angrite as a reference point to cross-calibrate the Mn–Cr and Pb–Pb systems. Thus, $^{53}\mathrm{Mn}/^{55}\mathrm{Mn} = 1.25 \times 10^{-6}$ is tied to an absolute Pb–Pb age of 4,557.8 Ma. By this reckoning, the ''global'' differentiation of the Howardite–Eucrite–Diogenite (HED) parent body is pinned by the ensemble eucrite Mn–Cr isochron to 4,565 Ma. As mentioned previously, individual eucrites show internal Mn–Cr isochrons that indicate attainment of isotopic closure from just slightly after this time to significantly later, implying an extended ($>10^7$ years) history of thermal activity on the HED asteroid. This is qualitatively in agreement with the young U–Pb ages of eucrites; however, a quantitative correlation between Mn–Cr and U–Pb ages is lacking (Tera and Carlson, 1999).

The ^{53}Mn–^{53}Cr isochron for the HED parent body is generally consistent with the timing of other indicators of early planetary processes. The Pb–Pb age for the oldest phosphates, from the least metamorphosed (H4) chondrites studied, postdates HED differentiation by $\sim$2 Myr. This is approximately equivalent to the Mn–Cr closure age for Chervony Kut, the noncumulate eucrite with the highest individual ^{53}Mn/^{55}Mn initial ratio. Other achondrites, including a pallasite and the unusual basaltic achondrite Acapulco, have Mn–Cr ages $\sim$8–10 Myr after the HED differentiation event. These timescales are consistent with the notion that a variety of differentiated meteorites sample various depths in asteroids of various sizes during this early epoch following accretion.

A problem arises with the apparent chronology of aqueous activity on carbonaceous chondrite parent bodies. The formation time of fayalite is reasonable from the Mn–Cr point of view; however, carbonates from CM chondrites and from the unique chondrite Kaidun have ^{53}Mn/^{55}Mn initial values commensurate with those of chondrules. Although we have argued above that there are problems in understanding the temporal meaning of Mn–Cr systematics in CAIs and chondrules, we note that if ^{53}Mn–^{53}Cr can serve as an accurate chronometer at least for chondrules, then it implies that aqueous activity on some chondrite parent bodies was contemporaneous with chondrule formation elsewhere. The data that exist thus far are for carbonates from carbonaceous chondrites and for chondrules from ordinary chondrites. There are no data to suggest that chondrules from carbonaceous chondrites might be older than those from ordinary chondrites; in fact limited Al–Mg data could be interpreted to suggest the opposite (Kunihiro *et al.*, 2004). Clearly, carbonates formed very early, but whether chondrule formation was still ongoing during this aqueous activity will have to be decided by further study, preferably of chondrules and secondary minerals from the same meteorites.

The experimental record documenting the prior existence of ^{26}Al in differentiated meteorites is mostly based on very recent data, the majority of which have only been published in abstract form. Certainly, the finding of $^{26}\mathrm{Mg}^*$ and of good Al–Mg isochrons in eucrites is consistent with the early age of igneous activity inferred from Mn–Cr systematics of bulk eucrites. This is strong confirmation that

planetary-scale melting began not more than a few million years following CAI crystallization, and quite possibly, while chondrule formation was still ongoing.

Amelin *et al.* (2006) have compared Pb–Pb, Al–Mg, and Mn–Cr ages for a number of differentiated meteorites, tying Pb–Pb with Al–Mg for CAIs and Pb–Pb with Mn–Cr for LEW86010 as we discuss above. They find internal consistency with two exceptions: the Pb–Pb ages of the Asuka 881394 eucrite and the Sahara 99555 angrite are ~3 Myr older than both Al–Mg and Mn–Cr ages. Amelin *et al.* (2006) suggest that this discordance may be caused by differences in closure temperatures of the three chronometers. Asuka 881394 has a slow cooling rate allowing this explanation, but mineralogical and textural indicators suggest that Sahara 99555 cooled too fast to allow a 3 Myr discordance in ages. Progress is being made in tying together long- and short-lived chronometers, but a completely self-consistent picture has not yet emerged.

1.16.7 CONCLUSIONS

Both chondrites and differentiated meteorites preserve records of short-lived radionuclides which are now-extinct, but which were present when the solar system formed (Table 1). These isotopic records yield information on the amount of radioactivity contained by ancient solar system minerals, from which the relative timing of chemical fractionations between parent and daughter elements can be inferred (assuming that the short-lived radionuclides were originally distributed homogenously). The fractionation events can often be related to thermal processes occurring in the solar nebula or on early-accreted planetesimals, thus allowing a high-resolution relative chronology to be delineated (Figure 10).

The existence of ^{10}Be, ^{36}Cl, and ^{60}Fe in various early solar system materials provides strong evidence for a multiplicity of sources for short-lived isotopes. The first two isotopes most likely result from local production by energetic particle irradiation, perhaps near the forming Sun, whereas the latter is evidence for seeding of the solar nebula by freshly synthesized stellar ejecta. In principle, the inventory of other radioisotopes may contain contributions from both these sources in addition to other nondiscrete (''background'') sources such as galactic stellar nucleosynthesis or spallogenic nuclear reactions in the protosolar molecular cloud. However, correlations of radiogenic isotope signatures in CAIs and hibonite grains indicate that spallogenic contributions to the abundances of the shortest-lived isotopes, ^{41}Ca and ^{26}Al, are minor and that these refractory isotopes arrived together in the solar nebula.

1.16.7.1 Implications for Solar Nebula Origin and Evolution

The short lifetimes of ^{26}Al and, especially, ^{41}Ca, coupled with the evidence for an external origin of these nuclides, have important implications for the origin of the solar system. On the basis of estimated production rates and isotope mixing during interstellar transit and injection into the solar system, a duration of at most ~1 Myr can be accommodated for the total time between nucleosynthetic production and incorporation of these isotopes into crystalline solids in the early solar system. Such a rapid timescale implies a triggering mechanism for fragmentation and collapse of a portion of the presolar molecular cloud to form the early Sun and its accretion disk. Although it is known that many AGB stars contributed dust to the early solar nebula (see Chapter 1.02) and that a wind from such a star could theoretically provide a sufficient shock to initiate collapse, astrophysical considerations of stellar lifetimes suggest a nearby type II supernova as a more likely trigger.

Supernovae can be the source of most of the short-lived radionuclides (except ^{10}Be); however there are difficulties in reconciling relative abundances of all species with a single event (see review by Goswami and Vanhala, 2000). While this may be aesthetically desirable, it is not required, especially for the longer-lived isotopes of Table 1. Other evidence indicates that it is probably not correct and that the truth is more complex than a single supernova triggering and injection. The ''last'' supernova is not the source of large stable isotope anomalies in oxygen, calcium, or titanium, demonstrating that isotopic memories of other presolar components survived to be incorporated into early solar system minerals. Additionally, the evidence for pervasive ^{10}Be signatures in CAIs, the strong hint for ^{7}Be, and the abundant astronomical evidence for copious X-ray activity of YSO indicate that early-formed solar system materials were most likely strongly irradiated if they were not shielded. Further work is required to quantitatively assess the proportion of those radionuclides (besides ^{26}Al) that were produced locally by solar energetic particles.

Cross-calibration of the initial ^{26}Al/^{27}Al records inferred for nebular components of chondrites with the absolute Pb–Pb ages of CAIs results in a self-consistent high-resolution

chronology for the high-temperature phases of solar nebula evolution. A plausible scenario and timeline can be constructed:

1. at nearly 4,568 Ma, a shock wave, probably initiated by a "nearby" supernova, triggers fragmentation and gravitational collapse of a portion of a molecular cloud;
2. near the central, hot regions of the nebula the first refractory minerals form by evaporation and/or recondensation and melting of mixtures of presolar dust grains from various interstellar heritages; these hibonite grains and FUN inclusions incorporate ^{10}Be produced by irradiation of the dust grains by solar energetic particles, but they do not sample the radioactivity accompanying the supernova shock wave;
3. shortly afterward, at ~4,567 Ma, the fresh radioactivity arrives in the inner nebula and most CAIs form over a short interval incorporating ^{26}Al and ^{41}Ca; if the new high-precision Al–Mg data on large CV CAIs is representative of most refractory inclusions, then this interval may be as short as 15 kyr;
4. high-temperature processing of some CAIs continues for a few hundred thousand years, but most of those that do not accrete to the Sun are removed from high-temperature regions of the nebula, perhaps by entrainment in bipolar outflows, and survive for a long period of time in undetermined nebular locations;
5. at ~4,566 Ma, chondrule formation begins and continues for ~1–2 Myr; CAIs are largely absent from the nebular regions where chondrule melting occurs; and
6. at ~4,565–4,564 Ma, CAIs have joined chondrules and nebular dust in accreting to planetesimals in the asteroid belt. If the latter process is considered as the termination of the nebular phase of solar system evolution, then its lifetime is ~4 Ma as recorded by radionuclides in nebular materials.

The timescales for accretion and early evolution of these planetesimals are also constrained by short-lived radioactivity. This record is best elucidated with the ^{53}Mn–^{53}Cr isotopic system, even though as discussed previously the record of ^{53}Mn/^{55}Mn in solar nebula objects does not yield a consistently interpretable chronology. The ^{182}Hf–^{182}W isotopic system indicates that core separation on differentiated meteorites occurred within 1 Myr of CAI formation. Accretion of some planetesimals started very early, perhaps even before the bulk of chondrule formation began. By ~4,565–4,564 Ma, large-scale melting and differentiation occurred on the HED parent body, most likely the asteroid 4 Vesta. Some eucrites crystallized soon after mantle differentiation, quickly cooling through isotopic closure for magnesium and chromium by ~4,564–4,563 Ma. Energy from ^{26}Al and ^{60}Fe decay probably contributed substantially to the heat required for melting, but the asteroid was large enough that igneous activity continued for several tens of million years. Some angrites appear to have erupted early, cooling by ~4,561 Ma, but ADOR and LEW did not crystallize until 4,558 Ma. Other asteroidal bodies, from which chondrites are derived, either accreted somewhat later than Vesta or remained as relatively small bodies for several million years. Absolute Pb–Pb ages of phosphates indicate that metamorphic temperatures were reached on some ordinary chondrite asteroids by ~4,563 Ma; this timescale is consistent with the ^{26}Al/^{27}Al records of chondrules. Metamorphism on chondrite parent bodies continued for up to tens of millions of years as indicated by Pb–Pb and I–Xe dating. Aqueous activity (formation of carbonate) happened very early, perhaps "too" early, on the parent asteroids of some carbonaceous chondrites. Calibration of the ^{53}Mn–^{53}Cr chronometer by the Pb–Pb age of angrites implies formation of the earliest of these carbonates by ~4,567 Ma, which is not compatible with the nebular chronology discussed above. Accretion and differentiation of planetary embryos continued from this early epoch for a period of several tens of millions of years (see Chapters 1.17 and 1.20).

1.16.7.2 Future Directions

The quantitative comparison of various short-lived radionuclide systems with each other and with Pb–Pb chronology has only been made possible by new data obtained during the last decade, or in many cases, the last few years. Over this same time period, evidence for the decay of several important new short-lived isotopes in the early solar system has been discovered. The record of now-extinct isotopes in early solar system materials is becoming sufficiently well defined to allow construction of a plausible timeline and scenario for solar system origin. However, even though broad areas of consistency have been revealed, there are significant problems that will require further investigation. One of the most important is trying to understand the role of energetic particle irradiation in the early solar system. Energetic processes associated with magnetic

flare activity of the young Sun almost certainly occurred; the question is what effect these had on isotopic and mineralogical records of early-formed solar system rocks. Could solar system irradiation be responsible for some of the confusion of the nebular record of $^{53}Mn/^{55}Mn$? There appears to be large-scale inhomogeneity in the ^{53}Mn–^{53}Cr systematics: could some of this be explicable in terms of solar system production and/or large-scale radial transport of nebular components? Or, is $^{53}Mn/^{55}Mn$ homogeneous after all (Trinquier *et al.*, 2005b)?

It has been recently hypothesized (Desch *et al.*, 2004) that ^{10}Be may result from magnetic trapping of cosmic radiation in molecular cloud material, such that all short-lived nuclides predate solar system formation. However, little attention has so far been paid to the role of magnetic fields in triggered collapse mechanisms. It is clear that magnetic pressure cannot substantially inhibit collapse, otherwise the delay would cause extinction of the signal of ^{41}Ca in CAIs. The correlation of ^{41}Ca with ^{26}Al needs to be better quantified, and even the canonical ^{26}Al record more closely examined to sort out the intrinsic dispersion in the distribution from the effects of secondary heating and alteration of CAI minerals. As it stands, the duration of CAI production seems implausibly short compared with CAI longevity in the nebula, but this is largely a model-dependent result. A better understanding of the locales and formation mechanisms of CAIs and chondrules, and their relationships to each other, will help in constraining such models. Finally, it can be anticipated that in the near future much more data will be gathered by *in situ* methods and high-precision bulk methods that will greatly improve our knowledge of the distributions of ^{10}Be and ^{60}Fe in a wide range of early materials. So far, these isotopes have been primarily exploited as semiquantitative indicators of process; perhaps with a more robust data set, it will be possible to employ them as further chronological tools for understanding solar nebula origin and evolution.

ACKNOWLEDGMENTS

We thank Y. Amelin, G. Huss, G. J. MacPherson, and S. Tachibana for providing figures and data used herein.

REFERENCES

Alexander C. M. O. D., Boss A. P., and Carlson R. W. (2001) The early evolution of the inner solar system: a meteoritic perspective. *Science* **293**, 64–68.

Allègre C. J., Manhès G., and Göpel C. (1995) The age of the Earth. *Geochim. Cosmochim. Acta* **59**, 1445–1456.

Amelin Y. (2006) The prospect of high-precision Pb isotopic dating of meteorites. *Meteorit. Planet. Sci.* **41**, 7–17.

Amelin Y., Krot A. N., Hutcheon I. D., and Ulyanov A. A. (2002) Lead isotopic ages of chondrules and calcium–aluminum-rich inclusions. *Science* **297**, 1678–1683.

Amelin Y., Wadhwa M., and Lugmair G. W. (2006) Pb-isotopic dating of meteorites using ^{202}Pb–^{205}Pb double spike: comparison with other high resolution chronometers. In *Lunar Planet. Sci.* **XXXVII**, #1970. The Lunar and Planetary Institute, Houston (CD-ROM).

André P., Ward-Thompson W., and Barsony M. (2000) From prestellar cores to protostars: the initial conditions of star formation. In *Protostars and Planets IV* (eds. V. Mannings, A. P. Boss, and S. S. Russell). University of Arizona Press, Tucson, AZ, pp. 59–96.

Baker J., Bizzarro M., Wittig N., Connelly J., and Haack H. (2005) Early planetesimal melting from an age of 4.5662 Gyr for differentiated meteorites. *Nature* **436**, 1127–1130.

Begemann F. (1980) Isotopic anomalies in meteorites. *Rep. Prog. Phys.* **43**, 1309–1356.

Binzel R. P. and Xu S. (1993) Chips off of asteroid 4 Vesta: evidence for the parent body of basaltic achondrite meteorites. *Science* **260**, 186–191.

Birck J. L. and Allègre C. J. (1985) Evidence for the presence of Mn-53 in the early solar-system. *Geophys. Res. Lett.* **12**, 745–748.

Birck J. L. and Allègre C. J. (1988) Manganese–chromium isotope systematics and the development of the early solar-system. *Nature* **331**, 579–584.

Birck J. L. and Lugmair G. W. (1988) Nickel and chromium isotopes in Allende inclusions. *Earth Planet. Sci. Lett.* **90**, 131–143.

Birck J. L., Rotaru M., and Allègre C. J. (1999) ^{53}Mn–^{53}Cr evolution of the early solar system. *Geochim. Cosmochim. Acta* **63**, 4111–4117.

Bizzarro M., Baker J. A., and Haack H. (2004) Mg isotope evidence for contemporaneous formation of chondrules and refractory inclusions. *Nature* **431**, 275–278.

Bizzarro M., Baker J. A., and Haack H. (2005) Corrigendum to Bizzarro *et al.* (2004). *Nature* **435**, 1280.

Bizzarro M., Ulfbeck D., and Thrane K. (2006) Nickel isotopes in meteorites: evidence for live ^{60}Fe and distinct ^{62}Ni isotope reservoirs in the early solar system. In *Lunar Planet. Sci.* **XXXVII**, #2020. The Lunar and Planetary Institute, Houston (CD-ROM).

Boss A. P. and Vanhala H. A. T. (2001) Injection of newly synthesized elements into the protosolar cloud. *Phil. Trans. Roy Soc. Lond. A* **359**, 2005–2016.

Brazzle R. H., Pravdivtseva O. V., Meshik A. P., and Hohenberg C. M. (1999) Verification and interpretation of the I–Xe chronometer. *Geochim. Cosmochim. Acta* **63**, 739–760.

Busso M., Gallino R., and Wasserburg G. J. (1999) Nucleosynthesis in asymptotic giant branch stars: relevance for galactic enrichment and solar system formation. *Annu. Rev. Astron. Astrophys.* **37**, 239–309.

Caillet C., MacPherson G. J., and Zinner E. K. (1993) Petrologic and Al–Mg isotopic clues to the accretion of two refractory inclusions onto the Leoville parent body: one was hot, the other wasn't. *Geochim. Cosmochim. Acta* **57**, 4725–4743.

Cameron A. G. W. (1995) The first ten million years in the solar nebula. *Meteorit. Planet. Sci.* **30**, 133–161.

Cameron A. G. W. (2001a) Extinct radioactivities, core-collapse supernovas, jets, and the r-process. *Nucl. Phys. A* **688**, 289C–296C.

Cameron A. G. W. (2001b) Some properties of r-process accretion disks and jets. *Astrophys. J.* **562**, 456–469.

Cameron A. G. W., Höflich P., Myers P. C., and Clayton D. D. (1995) Massive supernovae, Orion gamma rays, and the formation of the solar system. *Astrophys. J.* **447**, L53–L57.

Cameron A. G. W. and Truran J. W. (1977) The supernova trigger for formation of the solar system. *Icarus* **30**, 447–461.

Carlson R. W. and Hauri E. (2001) Extending the ^{107}Pd–^{107}Ag chronometer to low Pd/Ag meteorites with MC-ICP-MS. *Geochim. Cosmochim. Acta* **65**, 1839–1848.

Chaussidon M., Robert F., Mangin D., Hanon P., and Rose E. F. (1997) Analytical procedures for the measurement of boron isotope compositions by ion microprobe in meteorites and mantle rocks. *Geostand. Newslett.* **21**, 7–17.

Chaussidon M., Robert F., and McKeegan K. D. (2006) Li and B isotopic variations in an Allende CAI: evidence for the *in situ* decay of short-lived ^{10}Be and for the possible presence of the short-lived nuclide ^{7}Be in the early solar system. *Geochim. Cosmochim. Acta* **70**, 224–245.

Chaussidon M., Robert F., Russell S. S., Gounelle M., and Ash R. D. (2003) Variations of apparent ^{10}Be/^{9}Be ratios in Leoville MRS-06 type B1 CAI: constraints on the origin of ^{10}Be and ^{26}Al. In *Lunar Planet. Sci.* **XXXIV**, #1347. The Lunar and Planetary Institute, Houston (CD-ROM).

Chen J. H., Papanastassiou D. A., and Wasserburg G. J. (2002) Re–Os and Pd–Ag systematics in group IIIAB irons and in pallasites. *Geochem. Cosmochim. Acta* **66**, 3793–3810.

Chen J. H. and Wasserburg G. J. (1980) A search for isotopic anomalies in uranium. *Geophys. Res. Lett.* **7**, 275–278.

Chen J. H. and Wasserburg G. J. (1981) The isotopic composition of uranium and lead in Allende inclusions and meteorite phosphates. *Earth Planet. Sci. Lett.* **52**, 1–15.

Chen J. H. and Wasserburg G. J. (1987) A search for evidence of extinct lead 205 in iron meteorites. *Lunar Planet. Sci.* **XVIII**, 165–166.

Chen J. H. and Wasserburg G. J. (1990) The isotopic composition of Ag in meteorites and the presence of ^{107}Pd in protoplanets. *Geochim. Cosmochim. Acta* **54**, 1729–1743.

Chen J. H. and Wasserburg G. J. (1996) Live ^{107}Pd in the early solar system and implications for planetary evolution. In *Earth Processes: Reading the Isotopic Code* (eds. A. Basu and S. Hart). Geophys. Monogr. 95. American Geophysical Union, Washington, DC, pp. 1–20.

Clayton D. D. (1982) Cosmic chemical memory—a new astronomy. *Quart. J. Roy. Astron. Soc.* **23**, 174–212.

Clayton D. D. (1986) Interstellar fossil ^{26}Mg and its possible relation to excess meteoritic ^{26}Mg. *Astrophys. J.* **310**, 490–498.

Clayton D. D., Dwek E., and Woosley S. E. (1977) Isotopic anomalies and proton irradiation in the early solar system. *Astrophys. J.* **214**, 300–315.

Clayton R. N. and Mayeda T. K. (1984) The oxygen isotope record in Murchison and other carbonaceous chondrites. *Earth Planet. Sci. Lett.* **67**, 151–161.

Cook D. L., Wadhwa M., Clayton R. N., Janney P. E., Dauphas N., and Davis A. M. (2005) Nickel isotopic composition of meteoritic metal: implications for the initial ^{60}Fe/^{56}Fe ratio in the early solar system. *Meteorit. Planet. Sci.* **40**, A33.

Cook D. L., Wadhwa M., Janney P. E., Dauphas N., Clayton R. N., and Davis A. M. (2006) High precision measurements of nickel isotopes in metallic samples via multi-collector ICPMS. *Anal. Chem.* (submitted).

Cosarinsky M., Taylor D. J., and McKeegan K. D. (2006) Aluminum-26 model ages of hibonite and spinel from type A inclusions in CV chondrites. In *Lunar Planet. Sci.* **XXXVII**, #2357. The Lunar and Planetary Institute, Houston (CD-ROM).

Cosarinsky M., Taylor D. J., McKeegan K. D., and Hutcheon I. D. (2005) Mg isotopic study of Wark–Lovering rims in type A inclusions from CV chondrites: formation mechanisms and timing. *Meteorit. Planet. Sci.* **40**, A34.

Cuzzi J. N., Davis S. S., and Dobrovolskis A. R. (2003) Creation and distribution of CAIs in the protoplanetary nebula. In *Lunar Planet. Sci.* **XXXIV**, #1749. The Lunar and Planetary Institute, Houston (CD-ROM).

Dauphas N., Foley C. N., Wadhwa M., Davis A. M., Janney P. E., Qin L., Göpel C., and Birck J.-L. (2005) Protracted core differentiation in asteroids from ^{182}Hf–^{182}W systematics in the Eagle Station pallasite. In *Lunar Planet. Sci.* **XXXVI**, #1100. The Lunar and Planetary Institute, Houston (CD-ROM).

Davis A. M., Richter F. M., Mendybaev R. A., Janney P. E., Wadhwa M., and McKeegan K. D. (2005) Isotopic mass fractionation laws and the initial solar system ^{26}Al/^{27}Al ratio. In *Lunar Planet. Sci.* **XXXVI**, #2334. The Lunar and Planetary Institute, Houston (CD-ROM).

Desch S. J., Connolly H. C., Jr., and Srinivasan G. (2004) An interstellar origin for the beryllium 10 in calcium-rich, aluminum-rich inclusions. *Astrophys. J.* **602**, 528–542.

Endress M., Zinner E., and Bischoff A. (1996) Early aqueous activity on primitive meteorite parent bodies. *Nature* **379**, 701–703.

Fahey A. J., Goswami J. N., McKeegan K. D., and Zinner E. (1987) ^{26}Al, ^{244}Pu, ^{50}Ti, REE, and trace element abundances in hibonite grains from CM and CV meteorites. *Geochim. Cosmochim. Acta* **51**, 329–350.

Feigelson E. D., Broos P., Gaffney J. A., Garmire G., Hillenbrand L. A., Pravdo S. H., Townsley L., and Tsuboi Y. (2002a) X-ray emitting young stars in the Orion Nebula. *Astrophys. J.* **574**, 258–292.

Feigelson E. D., Garmire G. P., and Pravdo S. H. (2002b) Magnetic flaring in the pre main-sequence sun and implications for the early solar system. *Astrophys. J.* **572**, 335–349.

Foster P. N. and Boss A. P. (1997) Injection of radioactive nuclides from the stellar source that triggered the collapse of the presolar nebula. *Astrophys. J.* **489**, 346–357.

Galer S. J. G. and Lugmair G. W. (1996) Lead isotope systematics of non-cumulate eucrites. *Meteoritics* **31**, A47–A48.

Galy A., Hutcheon I. D., and Grossman L. (2004) $(^{26}\mathrm{Al}/^{27}\mathrm{Al})_0$ of the solar nebula inferred from Al–Mg systematics in bulk CAIs from CV3 chondrites. In *Lunar Planet. Sci.* **XXXV**, #2334. The Lunar and Planetary Institute, Houston (CD-ROM).

Galy A., Young E. D., Ash R. D., and O'Nions R. K. (2000) The formation of chondrules at high gas pressures in the solar nebula. *Science* **290**, 1751–1753.

Gilmour J. D. (2000) The extinct radionuclide timescale of the solar system. *Space Sci. Rev.* **192**, 123–132.

Gilmour J. D. and Saxton J. M. (2001) A timescale of formation of the first solids. *Phil. Trans. Roy Soc. Lond. A* **359**, 2037–2048.

Göpel C., Manhès G., and Allègre C. J. (1994) U–Pb systematics of phosphates from equilibrated ordinary chondrites. *Earth Planet. Sci. Lett.* **121**, 153–171.

Goswami J. N., Marhas K. K., and Sahijpal S. (2001) Did solar energetic particles produce the short-lived nuclides present in the early solar system? *Astrophys. J.* **549**, 1151–1159.

Goswami J. N. and Vanhala H. A. T. (2000) Extinct radionuclides and the origin of the solar system. In *Protostars and Planets IV* (eds. V. Mannings, A. P. Boss, and S. S. Russell). University of Arizona Press, Tucson, AZ, pp. 963–994.

Gounelle M., Shu F. H., Shang H., Glassgold A. E., Rehm K. E., and Lee T. (2001) Extinct radioactivities and protosolar cosmic rays: self-shielding and light elements. *Astrophys. J.* **548**, 1051–1070.

Gray C. M. and Compston W. (1974) Excess ^{26}Mg in the Allende meteorite. *Nature* **251**, 495–497.

Grimm R. E. and McSween H. Y. (1994) Heliocentric zoning of the asteroid belt by aluminum-26 heating. *Science* **259**, 653–655.

Guan Y., Huss G. R., MacPherson G. J., and Wasserburg G. J. (2000) Calcium–aluminum-rich inclusions from enstatite chondrites: indigenous or foreign? *Science* **289**, 1330–1333.

Halliday A. and Lee D. C. (1999) Tungsten isotopes and the early development of the Earth and Moon. *Geochim. Cosmochim. Acta* **63**, 4157–4179.

Harper C. L., Jr. (1996) Evidence for ^{92g}Nb in the early solar system and evaluation of a new p-process cosmochronometer from ^{92g}Nb/^{92}Mo. *Astrophys. J.* **466**, 437–456.

Hester J. J., Desch S. J., Healy K. R., and Leshin L. A. (2004) The cradle of the solar system. *Science* **304**, 1116–1117.

Heymann D. and Dziczkaniec M. (1976) Early irradiation of matter in the solar system: magnesium (proton, neutron) scheme. *Science* **191**, 79–81.

Hsu W., Guan Y., Leshin L. A., Ushikubo T., and Wasserburg G. J. (2006) A late episode of irradiation in the early solar system: evidence from extinct ^{36}Cl and ^{26}Al in meteorites. *Astrophys. J.* **640**, 525–529.

Hsu W., Huss G. R., and Wasserburg G. J. (2003) Al–Mg systematics of CAIs, POI, and ferromagnesian chondrules from Ningqiang. *Meteorit. Planet. Sci.* **38**, 35–48.

Hsu W. B., Wasserburg G. J., and Huss G. R. (2000) High time resolution by use of the Al-26 chronometer in the multistage formation of a CAI. *Earth Planet. Sci. Lett.* **182**, 15–29.

Hua J., Huss G. R., and Sharp T. G. (2002) ^{53}Mn–^{53}Cr dating of fayalite formation in the Kaba CV3 carbonaceous chondrite. *Lunar Planet. Sci.* **XXXIII**, 1660.

Hudson G. B., Kennedy B. M., Podosek F. A., and Hohenberg C. M. (1988) The early solar system abundance of ^{244}Pu as inferred from the St. Severin chondrite. *Proc. 19th Lunar Planet. Sci. Conf.* pp. 547–557.

Huss G. R., MacPherson G. J., Wasserburg G. J., Russell S. S., and Srinivasan G. (2001) Aluminum-26 in calcium–aluminum-rich inclusions and chondrules from unequilibrated ordinary chondrites. *Meteorit. Planet. Sci.* **36**, 975–997.

Hutcheon I. D., Armstrong J. T., and Wasserburg G. J. (1984) Excess ^{41}K in Allende CAI: confirmation of a hint. In *Lunar Planet. Sci.* The Lunar and Planetary Institute, Houston, pp. 387–388.

Hutcheon I. D., Browning L., Keil K., Krot A. N., Phinney D. L., Prinz M., and Weisberg M. K. (1999a) Timescale of aqueous activity in the early solar system. In *Ninth Goldschmidt Conf. Abstr.*, #971. Lunar and Planetary Institute, Houston (CD-ROM).

Hutcheon I. D., Huss G. R., and Wasserburg G. J. (1994) A search for ^{26}Al in chondrites: chondrule formation times. In *Lunar Planet. Sci.* The Lunar and Planetary Institute, Houston, pp. 587–588.

Hutcheon I. D. and Hutchison R. (1989) Evidence from the Semarkona ordinary chondrite for ^{26}Al heating of small planets. *Nature* **337**, 238–241.

Hutcheon I. D. and Jones R. H. (1995) The ^{26}Al–^{26}Mg record of chondrules: clues to nebular chronology. In *Lunar Planet. Sci.* The Lunar and Planetary Institute, Houston, pp. 647–648.

Hutcheon I. D., Krot A. N., Keil K., Phinney D. L., and Scott E. R. D. (1998) ^{53}Mn–^{53}Cr dating of fayalite formation in the CV3 chondrite Mokoia: evidence for asteroidal alteration. *Science* **282**, 1865–1867.

Hutcheon I. D. and Phinney D. L. (1996) Radiogenic ^{53}Cr* in Orgueil carbonates: chronology of aqueous activity on the CI parent body. In *Lunar Planet. Sci.* The Lunar and Planetary Institute, Houston, pp. 577–578.

Hutcheon I. D., Weisberg M. K., Phinney D. L., Zolensky M. E., Prinz M., and Ivanov A. V. (1999b) Radiogenic ^{53}Cr in Kaidun carbonates: evidence for very early aqueous activity. In *Lunar Planet. Sci.* **XXX**, #1722. The Lunar and Planetary Institute, Houston (CD-ROM).

Ireland T. R. (1988) Correlated morphological, chemical, and isotopic characteristics of hibonites from the Murchison carbonaceous chondrite. *Geochim. Cosmochim. Acta* **52**, 2827–2839.

Ireland T. R. (1990) Presolar isotopic and chemical signatures in hibonite-bearing refractory inclusions from the Murchison carbonaceous chondrite. *Geochim. Cosmochim. Acta* **54**, 3219–3237.

Ireland T. R., Compston W., and Heydegger H. R. (1985) Titanium isotopic anomalies in hibonites from the Murchison carbonaceous chondrite. *Geochim. Cosmochim. Acta* **49**, 1989–1993.

Jeffery P. M. and Reynolds J. H. (1961) Origin of excess Xe^{129} in stone meteorites. *J. Geophys. Res.* **66**, 3582–3583.

Kaiser T. and Wasserburg G. J. (1983) The isotopic composition and concentration of Ag in iron meteorites. *Geochim. Cosmochim. Acta* **47**, 43–58.

Kelly W. R. and Wasserburg G. J. (1978) Evidence for the existence of ^{107}Pd in the early solar system. *Geophys. Res. Lett.* **5**, 1079–1082.

Kita N. T., Huss G. R., Tachibana S., Amelin Y., Nyquist L. E., and Hutcheon I. D. (2005) Constraints on the origin of chondrules and CAIs from short-lived and long-lived radionuclides. In *Chondrites and the Protoplanetary Disk* (eds. A. N. Krot, E. R. D. Scott, and B. Reipurth), Astron. Soc. Pacific Conf. Ser. 341. Astronomical Society of the Pacific, San Francisco, pp. 558–587.

Kita N. T., Ikeda Y., Shimoda H., Morshita Y., and Togashi S. (2003) Timing of basaltic volcanism in ureilite parent body inferred from the ^{26}Al ages of plagioclase-bearing clasts in DAG-319 polymict ureilite. In *Lunar Planet. Sci.* **XXXIV**, #1557. The Lunar and Planetary Institute, Houston (CD-ROM).

Kita N. T., Nagahara H., Togashi S., and Morshita Y. (2000) A short duration of chondrule formation in the solar nebula: evidence from ^{26}Al in Semarkona ferromagnesian chondrules. *Geochim. Cosmochim. Acta* **64**, 3913–3922.

Kleine T., Mezger K., Palme H., Scherer E., and Münker C. (2005a) Early core formation in asteroids and late accretion of chondrite parent bodies: evidence from ^{182}Hf–^{182}W in CAIs, metal-rich chondrites, and iron meteorites. *Geochim. Cosmochim. Acta* **69**, 5805–5818.

Kleine T., Mezger K., Palme H., Scherer E., and Münker C. (2005b) The W isotope composition of eucrite metals: constraints on the timing and cause of thermal metamorphism of basaltic eucrites. *Earth Planet. Sci. Lett.* **231**, 41–52.

Kleine T., Munker C., Mezger K., and Palme H. (2002a) Rapid accretion and early core formation on asteroids and the terrestrial planets from Hf–W chronometry. *Nature* **418**, 952–955.

Kleine T., Munker C., Mezger K., Palme H., and Bischoff A. (2002b) Revised Hf–W ages for core formation in planetary bodies. *Geochim. Cosmochim. Acta* **66** A404–A404.

Krot A. N., Amelin Y., Cassen P., and Meibom A. (2005) Young chondrules in CB chondrites from a giant impact in the early solar system. *Nature* **436**, 989–992.

Krot A. N., McKeegan K. D., Leshin L. A., MacPherson G. J., and Scott E. R. D. (2002) Existence of an ^{16}O-rich gaseous reservoir in the solar nebula. *Science* **295**, 1051–1054.

Kunihiro T., Rubin A. E., McKeegan K. D., and Wasson J. T. (2004) Initial ^{26}Al/^{27}Al in carbonaceous-chondrite chondrules: too little ^{26}Al to melt asteroids. *Geochim. Cosmochim. Acta* **68**, 2947–2957.

LaTourrette T. and Wasserburg G. J. (1998) Mg diffusion in anorthite: implications for the formation of early solar system planetesimals. *Earth Planet. Sci. Lett.* **158**, 91–108.

Lee D. C. and Halliday A. N. (1996) Hf–W isotopic evidence for rapid accretion and differentiation in the early solar system. *Science* **274**, 1876–1879.

Lee T. (1978) A local proton irradiation model for isotopic anomalies in the solar system. *Astrophys. J.* **224**, 217–226.

Lee T., Mayeda T. K., and Clayton R. N. (1980) Oxygen isotopic anomalies in Allende inclusion HAL. *Geophys. Res. Lett.* **7**, 493–496.

Lee T. and Papanastassiou D. A. (1974) Mg isotopic anomalies in the Allende meteorite and correlation with O and Sr effects. *Geophys. Res. Lett.* **1**, 225–228.

Lee T., Papanastassiou D. A., and Wasserburg G. J. (1976) Demonstration of ^{26}Mg excess in Allende and evidence for ^{26}Al. *Geophys. Res. Lett.* **3**, 109–112.

Lee T., Papanastassiou D. A., and Wasserburg G. J. (1977) Aluminum-26 in the early solar system: fossil or fuel? *Astrophys. J* **211**, L107–L110.

Lee T., Russell W. A., and Wasserburg G. J. (1978) Calcium isotopic anomalies and the lack of aluminum-26 in an unusual Allende inclusion. *Astrophys. J.* **228**, L93–L98.

Lee T., Shu F. H., Shang H., Glassgold A. E., and Rehm K. E. (1998) Protostellar cosmic rays and extinct radioactivities in meteorites. *Astrophys. J.* **506**, 898–912.

Leya I., Halliday A. N., and Wieler R. (2003) The predictable collateral consequences of nucleosynthesis by spallation reactions in the early solar system. *Astrophys. J.* **594**, 605–616.

Lin Y., Guan Y., Leshin L. A., Ouyang Z., and Daode W. (2005) Short-lived chlorine-36 in a Ca- and Al-rich inclusion from the Ningqiang carbonaceous chondrite. *Proc. Natl. Acad. Sci.* **102**, 1306–1311.

Liu M.-C., McKeegan K. D., and Davis A. M. (2006) Magnesium isotopic compositions of CM hibonite grains. In *Lunar Planet. Sci.* **XXXVII**, #2428. The Lunar and Planetary Institute, Houston (CD-ROM).

Lugmair G. W. and Galer S. J. G. (1992) Age and isotopic relationships among the angrites Lewis Cliff 86010 and Angra dos Reis. *Geochim. Cosmochim. Acta* **56**, 1673–1694.

Lugmair G. W., Shimamura T., Lewis R. S., and Anders E. (1983) Samarium-146 in the early solar system: evidence from neodymium in the Allende meteorite. *Science* **222**, 1015–1018.

Lugmair G. W. and Shukolyukov A. (1998) Early solar system timescales according to ^{53}Mn–^{53}Cr systematics. *Geochim. Cosmochim. Acta* **62**, 2863–2886.

Lugmair G. W. and Shukolyukov A. (2001) Early solar system events and timescales. *Meteorit. Planet. Sci.* **36**, 1017–1026.

MacPherson G. J. and Davis A. M. (1993) A petrologic and ion microprobe study of a Vigarano type B refractory inclusion: evolution by multiple stages of alteration and melting. *Geochim. Cosmochim. Acta* **57**, 231–243.

MacPherson G. J., Davis A. M., and Zinner E. K. (1995) The distribution of aluminum-26 in the early solar system—a reappraisal. *Meteoritics* **30**, 365–386.

MacPherson G. J. and Huss G. R. (2001) Extinct ^{10}Be in CAIs from Vigarano, Leoville, and Axtell. In *Lunar Planet. Sci.* **XXXII**, #1882. The Lunar and Planetary Institute, Houston (CD-ROM).

MacPherson G. J., Huss G. R., and Davis A. M. (2003) Extinct ^{10}Be in type A calcium–aluminum-rich inclusions from CV chondrites. *Geochim. Cosmochim. Acta* **67**, 3165–3179.

Marhas K. K. and Goswami J. N. (2003) Be–B systematics in CM and CV hibonites: implications for solar energetic particle production of short-lived nuclides in the early solar system. In *Lunar Planet. Sci.*, #1303. The Lunar and Planetary Institute, Houston (CD-ROM).

Marhas K. K., Goswami J. N., and Davis A. M. (2002) Short-lived nuclides in hibonite grains from Murchison: evidence for solar system evolution. *Science* **298**, 2182–2185.

Markowski A., Quitté G., Halliday A. N., and Kleine T. (2006) Tungsten isotopic compositions of iron meteorites: chronological constraints vs. cosmogenic effects. *Earth Planet. Sci. Lett.* **242**, 1–15.

McKeegan K. D., Chaussidon M., Krot A. N., Robert F., Goswami J. N., and Hutcheon I. D. (2001) Extinct radionuclide abundances in Ca, Al-rich inclusions from the CV chondrites Allende and Efremovka: a search for synchronicity. In *Lunar Planet. Sci.*, #2175. The Lunar and Planetary Institute, Houston (CD-ROM).

McKeegan K. D., Chaussidon M., and Robert F. (2000a) Incorporation of short-lived Be-10 in a calcium–aluminum-rich inclusion from the Allende meteorite. *Science* **289**, 1334–1337.

McKeegan K. D., Greenwood J. P., Leshin L. A., and Cosarinsky M. (2000b) Abundance of ^{26}Al in ferromagnesian chondrules of unequilibrated ordinary chondrites. In *Lunar Planet. Sci.* **XXXI**, #2009. The Lunar and Planetary Institute, Houston (CD-ROM).

McKeegan K. D. and Leshin L. A. (2001) Stable isotope variations in extraterrestrial materials. *Rev. Mineral. Geochem.* **43**, 279–318.

Meyer B. and Clayton D. D. (2000) Short-lived radioactivities and the birth of the Sun. *Space Sci. Rev.* **92**, 133–152.

Mostefaoui S., Kita N. T., Togashi S., Tachibana S., Nagahara H., and Morishita Y. (2002) The relative formation ages of ferromagnesian chondrules inferred from their initial aluminum-26/aluminum-27 ratios. *Meteorit. Planet. Sci.* **37**, 421–438.

Mostefaoui S., Lugmair G. W., and Hoppe P. (2005) ^{60}Fe: a heat source for planetary differentiation from a nearby supernova explosion. *Astrophys. J.* **625**, 271–277.

Moynier F., Telouk P., and Albarede F. (2005) Excesses of ^{60}Ni in chondrites and iron meteorites. In *Lunar Planet. Sci.* **XXXVI**, #1593. The Lunar and Planetary Institute, Houston (CD-ROM).

Münker C., Weyer S., Mezger K., Rehkämper M., Wombacher F., and Bischoff A. (2000) ^{92}Nb–^{92}Zr and the early differentiation history of planetary bodies. *Science* **289**, 1538–1542.

Murty S. V. S., Goswami J. N., and Shukolyukov Y. A. (1997) Excess Ar-36 in the Efremovka meteorite: a strong hint for the presence of Cl-36 in the early solar system. *Astrophys. J.* **475**, L65–L68.

National Nuclear Data Center, http://www.nndc.bnl.gov (accessed on August 2006).

Niederer F. R., Papanastassiou D. A., and Wasserburg G. J. (1980) Endemic isotopic anomalies in titanium. *Astrophys. J.* **240**, L73–L77.

Nielsen S. G., Rehkämper M., and Halliday A. N. (2006) Large thallium isotopic variations in iron meteorites and evidence for lead-205 in the early solar system. *Geochim. Cosmochim. Acta* **70**, 2643–2657.

Niemeyer S. and Lugmair G. W. (1981) Ubiquitous isotopic anomalies in Ti from normal Allende inclusions. *Earth Planet. Sci. Lett.* **53**, 211–225.

Nyquist L., Lindstrom D., Mittlefehldt D., Shih C. Y., Wiesmann H., Wentworth S., and Martinez R. (2001a) Manganese–chromium formation intervals for chondrules from the Bishunpur and Chainpur meteorites. *Meteorit. Planet. Sci.* **36**, 911–938.

Nyquist L. E., Reese Y., Wiesmann H., Shih C.-Y., and Takeda H. (2001b) Live ^{53}Mn and ^{26}Al in a unique cumulate eucrite with very calcic feldspar (An-98). *Meteorit. Planet. Sci.* **36**, A151–A152.

Nyquist L. E., Shih C.-Y., Wiesmann H., and Mikouchi T. (2003) Fossil ^{26}Mg and ^{53}Mn in D'Orbigny and Sahara 99555 and the timescale for angrite magmatism. In *Lunar Planet. Sci.* **XXXIV**, #1338. The Lunar and Planetary Institute, Houston (CD-ROM).

Ouellette N., Desch S. J., Hester J. J., and Leshin L. A. (2005) A nearby supernova injected short-lived radionuclides into our protoplanetary disk. In *Chondrites and the Protoplanetary Disk* (eds. A. N. Krot, E. R. D. Scott, and B. Reipurth), Astron. Soc. Pacific Conf. Ser. 341. Astronomical Society of the Pacific, San Francisco, pp. 527–538.

Papanastassiou D. A. (1986) Chromium isotopic anomalies in the Allende meteorite. *Astrophys. J.* **308**, L27–L30.

Papanastassiou D. A., Bogdanovski O., and Wasserburg G. J. (2002) ^{53}Mn–^{53}Cr systematics in Allende refractory inclusions. *Meteorit. Planet. Sci.* **37**, A114.

Podosek F. A. and Cassen P. (1994) Theoretical, observational, and isotopic estimates of the lifetime of the solar nebula. *Meteoritics* **29**, 6–25.

Podosek F. A. and Nichols R. H., Jr. (1997) Short-lived radionuclides in the solar nebula. In *Astrophysical Implications of the Laboratory Study of Presolar Materials* (eds. T. J. Bernatowicz and E. Zinner). American Institute of Physics, Woodbury, pp. 617–647.

Podosek F. A., Ott U., Brannon J. C., Neal C. R., Bernatowicz T. J., Swan P., and Mahan S. (1997) Thoroughly anomalous chromium in Orgueil. *Meteorit. Planet. Sci.* **32**, 617–627.

Podosek F. A. and Swindle T. D. (1988) Extinct radionuclides. In *Meteorites and the Early Solar System* (eds. J. F. Kerridge and M. S. Matthews). University of Arizona Press, Tucson, AZ, pp. 1093–1113.

Podosek F. A., Zinner E., MacPherson G. J., Lundberg L. L., Brannon J. C., and Fahey A. J. (1991) Correlated study of initial ^{87}Sr/^{86}Sr and Al–Mg isotopic systematics and petrologic properties in a suite of refractory inclusions from the Allende meteorite. *Geochim. Cosmochim. Acta* **55**, 1083–1110.

Preibisch T., Kim Y. C., Favata F., Feigelson E. D., Flaccomio E., Getman K., Micela G., Sciortino S., Stassun K., Stelzer B., and Zinnecker H. (2005) The origin of T tauri X-ray emission: new insights from the Chandra Orion Ultradeep Project. *Astrophys. J. Suppl.* **160**, 401–422.

Prinzhofer A., Papanastassiou D. A., and Wasserburg G. J. (1989) The presence of ^{146}Sm in the early solar system and implications for its nucleosynthesis. *Astrophys. J.* **344**, 81–84.

Qin L., Dauphas N., Wadhwa M., Janney P. E., Davis A. M., and Mazarik J. (2006) Evidence of correlated cosmogenic effects in iron meteorites: implications for the timing of metal–silicate differentiation in asteroids. In *Lunar Planet. Sci.* **XXXVII**, #1771. The Lunar and Planetary Institute, Houston (CD-ROM).

Richter F. M., Davis A. M., DePaolo D. J., and Watson E. B. (2003) Isotope fractionation by chemical diffusion between molten basalt and rhyolite. *Geochim. Cosmochim. Acta* **67**, 3905–3923.

Rotaru M., Birck J.-L., and Allègre C. J. (1992) Clues to early solar system history from chromium isotopes in carbonaceous chondrites. *Nature* **358**, 465–470.

Russell S. S., Gounelle M., and Hutchison R. (2001) Origin of short-lived radionuclides. *Phil. Trans. Roy Soc. Lond.* **359**, 1991–2004.

Russell S. S., Srinivasan G., Huss G. R., Wasserburg G. J., and MacPherson G. J. (1996) Evidence for widespread ^{26}Al in the solar nebula and constraints for nebula timescales. *Science* **273**, 757–762.

Sahijpal S. and Goswami J. N. (1998) Refractory phases in primitive meteorites devoid of ^{26}Al and ^{41}Ca: representative samples of first solar system solids? *Astrophys. J.* **509**, L137–L140.

Sahijpal S., Goswami J. N., and Davis A. M. (2000) K, Mg, Ti, and Ca isotopic compositions and refractory trace element abundances in hibonites from CM and CV meteorites: implications for early solar system processes. *Geochim. Cosmochim. Acta* **64**, 1989–2005.

Sahijpal S., Goswami J. N., Davis A. M., Grossman L., and Lewis R. S. (1998) A stellar origin for the short-lived nuclides in the early solar system. *Nature* **391**, 559.

Sahijpal S., McKeegan K. D., Krot A. N., Weber D., and Ulyanov A. A. (1999) Oxygen isotopic compositions of Ca–Al-rich inclusions from the CH chondrites, Acfer 182 and Pat91546. *Meteorit. Planet. Sci.* **34**, A101.

Sanloup C., Blicher-Toft J., Télouk P., Gillet P., and Albarède F. (2000) Zr isotope anomalies in chondrites and the presence of ^{92}Nb in the early solar system. *Earth Planet. Sci. Lett.* **184**, 75–81.

Schönbachler M., Rehkämper M., Halliday A. N., Lee D.-C., Bourot-Denise M., Zanda B., Hattendorf B., and Günther D. (2002) Niobium–zirconium chronometry and early solar system development. *Science* **295**, 1705–1708.

Schramm D. N., Tera F., and Wasserburg G. J. (1970) The isotopic abundance of ^{26}Mg and limits on ^{26}Al in the early solar system. *Earth Planet. Sci. Lett.* **10**, 44–59.

Shu F. H., Adams F. C., and Lizano S. (1987) Star formation in molecular clouds: observation and theory. *Annu. Rev. Astron. Astrophys.* **25**, 23–81.

Shu F. H., Shang H., Gounelle M., Glassgold A. E., and Lee T. (2001) The origin of chondrules and refractory inclusions in chondritic meteorites. *Astrophys. J.* **548**, 1029–1050.

Shukolyukov A. and Lugmair G. W. (1993a) Fe-60 in eucrites. *Earth Planet. Sci. Lett.* **119**, 159–166.

Shukolyukov A. and Lugmair G. W. (1993b) Live iron-60 in the early solar system. *Science* **259**, 1138–1142.

Shukolyukov A. and Lugmair G. W. (1998) Isotopic evidence for the Cretaceous–Tertiary impactor and its type. *Science* **282**, 927–929.

Simon J. I., Young E. D., Russell S. S., Tonui E. K., Dyl K. A., and Manning C. E. (2005) A short timescale for changing oxygen fugacity in the solar nebula revealed by high-resolution ^{26}Al–^{26}Mg dating of CAI rims. *Earth Planet. Sci. Lett.* **238**, 272–283.

Srinivasan G. (2001) Be–B isotope systematics in CAI E65 from Efremovka CV3 chondrite. *Meteorit. Planet. Sci.* **36**, A195–A196.

Srinivasan G., Goswami J. N., and Bhandari N. (1999) Al-26 in eucrite Piplia Kalan: plausible heat source and formation chronology. *Science* **284**, 1348–1350.

Srinivasan G., Sahijpal S., Ulyanov A. A., and Goswami J. N. (1996) Ion microprobe studies of Efremovka CAIs: potassium isotope composition and ^{41}Ca in the early solar system. *Geochim. Cosmochim. Acta* **60**, 1823–1835.

Srinivasan G., Ulyanov A. A., and Goswami J. N. (1994) ^{41}Ca in the early solar system. *Astrophys. J.* **431**, L67–L70.

Stewart B. W., Papanastassiou D. A., and Wasserburg G. J. (1994) Sm–Nd chronology and petrogenesis of mesosiderites. *Geochim. Cosmochim. Acta* **58**, 3487–3509.

Stirling C. H., Halliday A. N., and Porcelli D. (2005) In search of live ^{247}Cm in the early solar system. *Geochim. Cosmochim. Acta* **69**, 1059–1071.

Sugiura N. (2001) Boron isotopic compositions in chondrules: anorthite-rich chondrules in the Yamato 82094 (CO3) chondrite. In *Lunar Planet. Sci.* **XXXII**, #1277. The Lunar and Planetary Institute, Houston (CD-ROM).

Sugiura N., Shuzou Y., and Ulyanov A. (2001) Beryllium–boron and aluminum–magnesium chronology of

calcium–aluminum-rich inclusions in CV chondrites. *Meteorit. Planet. Sci.* **36**, 1397–1408.

Swindle T. D., Caffee M. W., Hohenberg C. M., Lindstrom M. M., and Taylor G. J. (1991) Iodine–xenon studies of petrographically and chemically characterized Chainpur chondrules. *Geochim. Cosmochim. Acta* **55**, 861–880.

Swindle T. D., Davis A. M., Hohenberg C. M., MacPherson G. J., and Nyquist L. E. (1996) Formation times of chondrules and Ca–Al-rich inclusions: constraints from short-lived radionuclides. In *Chondrules and the Protoplanetary Disk 1996* (eds. R. H. Hewins, R. H. Jones, and E. R. D. Scott). Cambridge University Press, New York, pp. 77–86.

Tachibana S. and Huss G. R. (2003) The initial abundance of ^{60}Fe in the solar system. *Astrophys. J.* **588**, L41–L44.

Tachibana S., Huss G. R., Kita N. T., Shimoda G., and Morishita Y. (2006) ^{60}Fe in chondrites: debris from a nearby supernova in the early solar system? *Astrophys. J.* **639**, L87–L90.

Taylor D. J., Cosarinsky M., Liu M.-C., McKeegan K. D., Krot A. N., and Hutcheon I. D. (2005) Survey of initial ^{26}Al in type A and type B CAIs: evidence for an extended formation period for refractory inclusions. *Meteorit. Planet. Sci.* **40**, A151.

Tera F. and Carlson R. W. (1999) Assessment of the Pb–Pb and U–Pb chronometry of the early solar system. *Geochim. Cosmochim. Acta* **63**, 1877–1889.

Tera F. and Wasserburg G. J. (1972) U–Th–Pb systematics in three Apollo 14 basalts and the problem of initial lead in lunar rocks. *Earth Planet. Sci. Lett.* **14**, 281–304.

Tilton G. R. (1988) Age of the solar system. In *Meteorites and the Early Solar System* (eds. J. F. Kerridge and M. S. Matthews). University of Arizona Press, Tucson, AZ, pp. 259–275.

Trinquier A., Birck J.-L., and Allègre C. J. (2005a) ^{54}Cr anomalies in the solar system: their extent and origin. In *Lunar Planet. Sci.* **XXXVI**, #1259. The Lunar and Planetary Institute, Houston (CD-ROM).

Trinquier A., Birck J.-L., and Allègre C. J. (2005b) Reevaluation of the ^{53}Mn–^{53}Cr systematic in the basaltic achondrites. In *Lunar Planet. Sci.* **XXXVI**, #1946. The Lunar and Planetary Institute, Houston (CD-ROM).

Wadhwa M., Amelin Y., Bogdanovski O., Shukolyukov A., Lugmair G. W., and Janney P. (2005) High precision relative and absolute ages for Asuka 881394, a unique and ancient basalt. In *Lunar Planet. Sci.* **XXXVI**, #2126. The Lunar and Planetary Institute, Houston (CD-ROM).

Wadhwa M., Amelin Y., Davis A. M., Lugmair G. W., Meyer B., Gounelle M., and Desch S. J. (2006a) From dust to planetesimals: implications for the solar protoplanetary disk from short-lived radionuclides. In *Protostars and Planets V* (eds. B. Reipurth, D. Jewitt, and K. Keil). University of Arizona Press, Tucson, AZ.

Wadhwa M., Foley C. N., Janney P., and Beecher N. A. (2003) Magnesium isotopic composition of the Juvinas eucrite: implications for concordance of the Al–Mg and Mn–Cr chronometers and timing of basaltic volcanism on asteroids. In *Lunar Planet. Sci.* **XXXIV**, #2055. The Lunar and Planetary Institute, Houston (CD-ROM).

Wadhwa M. and Lugmair G. W. (1996) Age of the eucrite "Caldera" from convergence of long-lived and short-lived chronometers. *Geochim. Cosmochim. Acta* **60**, 4889–4893.

Wadhwa M. and Russell S. S. (2000) Timescales of accretion and differentiation in the early solar system: the meteoritic evidence. In *Protostars and Planets IV* (eds. V. Mannings, A. P. Boss, and S. S. Russell). University of Arizona Press, Tucson, AZ, pp. 995–1018.

Wadhwa M., Srinivasan G., and Carlson R. W. (2006b) Timescales of planetary differentiation in the early solar system. In *Meteorites and the Early Solar System II* (eds. D. S. Lauretta and H. Y. Jr. McSween). University of Arizona Press, Tucson, AZ, pp. 715–731.

Wadhwa M., Zinner E. K., and Crozaz G. (1997) Manganese–chromium systematics in sulfides of unequilibrated enstatite chondrites. *Meteorit. Planet. Sci.* **32**, 281–292.

Wasserburg G. J. (1985) Short-lived nuclei in the early solar system. In *Protostars and Planets II* (eds. D. C. Black and M. S. Matthews). University of Arizona Press, Tucson, AZ, pp. 703–737.

Wasserburg G. J., Busso M., and Gallino R. (1996) Abundances of actinides and short-lived nonactinides in the interstellar medium: diverse supernova sources for the r-processes. *Astrophys. J.* **466**, L109–L113.

Wasserburg G. J., Busso M., Gallino R., and Nollett K. M. (2006) Short-lived nuclei in the early solar system: possible AGB sources. *Nucl. Phys. A* (in press).

Wasserburg G. J., Busso M., Gallino R., and Raiteri C. M. (1994) Asymptotic giant branch stars as a source of short-lived radioactive nuclei in the solar nebula. *Astrophys. J.* **424**, 412–428.

Wasserburg G. J., Gallino R., and Busso M. (1998) A test of the supernova trigger hypothesis with Fe-60 and Al-26. *Astrophys. J.* **500**, L189–L193.

Wasserburg G. J. and Papanastassiou D. A. (1982) Some short-lived nuclides in the early solar system—a connection with the placental ISM. In *Essays in Nuclear Astrophysics* (ed. D. N. Schramm). Cambridge University Press, Cambridge, MA, pp. 77–140.

Weber D., Zinner E., and Bischoff A. (1995) Trace element abundances and magnesium, calcium, and titanium isotopic compositions of grossite-containing inclusions from the carbonaceous chondrite Acfer 182. *Geochim. Cosmochim. Acta* **59**, 803–823.

Weidenschilling S. J. (1977) Aerodynamics of solid bodies in the solar nebula. *Mon. Not. Roy. Astron. Soc.* **180**, 57–70.

Wetherill G. W. (1956) Discordant uranium–lead ages. *Trans. Am. Geophys. Union* **37**, 320–326.

Whitby J., Burgess R., Turner G., Gilmour J., and Bridges J. (2000) Extinct ^{129}I in halite from a primitive meteorite: evidence for evaporite formation in the early solar system. *Science* **288**, 1819–1821.

Whitby J., Gilmour J., Turner G., Prinz M., and Ash R. D. (2001) Iodine–xenon dating of chondrules from the Quinzhen and Kota enstatite chondrites. *Geochim. Cosmochim. Acta* **66**, 347–359.

Yin Q. Z., Jacobsen S. B., McDonough W. F., and Horn I. (2000) Supernova sources and the ^{92}Nb–^{92}Zr p-process chronometer. *Astrophys. J.* **535**, L49–L53.

Yin Q. Z., Jacobsen S. B., Yamashita K., Blichert-Toft J., Telouk P., and Albarede F. (2002) A short timescale for terrestrial planet formation from Hf–W chronometry of meteorites. *Nature* **418**, 949–952.

Young E. D. and Russell S. S. (1998) Oxygen reservoirs in the early solar nebula inferred from an Allende CAI. *Science* **282**, 452–455.

Young E. D., Galy A., and Nagahara H. (2002) Kinetic and equilibrium mass-dependent isotope fractionation laws in nature and their geochemical and cosmochemical significance. *Geochim. Cosmochim. Acta* **66**, 1095–1104.

Young E. D., Simon J. I., Galy A., Russell S. S., Tonui E., and Lovera O. (2005) Supra-canonical ^{26}Al/^{27}Al and the residence time of CAIs in the solar protoplanetary disk. *Science* **308**, 223–227.

Yurimoto H., Ito M., and Nagasawa H. (1998) Oxygen isotope exchange between refractory inclusion in Allende and solar nebula gas. *Science* **282**, 1874–1877.

Zhai M., Nakamura E., Shaw D. M., and Nakano T. (1996) Boron isotope ratios in meteorites and lunar rocks. *Geochim. Cosmochim. Acta* **60**, 4877–4881.

Zinner E. (1998) Stellar nucleosynthesis and the isotopic composition of presolar grains from primitive meteorites. *Annu. Rev. Earth Planet. Sci.* **26**, 147–188.

Zinner E., Fahey A. J., Goswami J. N., Ireland T. R., and McKeegan K. D. (1986) Large ^{48}Ca anomalies are associated with ^{50}Ti anomalies in Murchison and Murray hibonites. *Astrophys. J.* **311**, L103–L107.

Zinner E. and Göpel C. (2002) Aluminum-26 in H4 chondrites: implications for its production and its usefulness as a fine-scale chronometer for early solar system events. *Meteorit. Planet. Sci.* **37**, 1001–1013.

Treatise On Geochemistry
ISBN (set): 0-08-043751-6
pp. 1–38